

SHASTA RIVER FLOW, TEMPERATURE, AND DISSOLVED OXYGEN MODEL CALIBRATION TECHNICAL REPORT



Prepared for the
Information Center for the Environment
Department of Environmental Science & Policy
University of California, Davis
and the
North Coast Regional Water Quality Control Boards
by
Limor Geisler
University of California, Davis

With assistance from
Watercourse Engineering, Inc.
133 D Street, Suite F
Davis, CA, 95616
September 28, 2005

Table of Contents

1.0 Introduction.....	2
1.1 Task 1. Data Analysis and Selection of Calibration/ Validation Periods	3
2.0 Task 2. Model Selection	5
3.0 Task 3. Geometry Conversion	5
3.1 Task 3a: Converting to the Lamphear Hydrography for Measured Cross-sectional Geometry Locations.....	6
3.2 Task 3b: Converting locations of estimated elevation to the Lamphear Hydrography	7
3.3 Task 3c: Comparing cross-sections	9
3.4 Task 3d: Updating Model Node Locations in the Lamphear Hydrography	11
3.5 Task 3e: Calculating new river azimuths.....	12
3.6 Task 3f: Converting shading file.....	12
4.0 Task 4: Re-formatting the Hydrodynamic ADYN file	14
5.0 Task 5: Formatting the Water Quality RQUAL files.....	14
5.1 Task 5a: Boundary condition file (*.rib).....	14
5.1.1 Temperature	15
5.1.2 Dissolved Oxygen, NBOD, CBOD	16
5.2 Task 5b: Meteorology file (*.rim)	22
5.3 Task 5c: Water quality coefficients and initial conditions file (*.ric)	22
5.3.1 Rates, Constants, Coefficients and Other Model Parameters	22
5.3.2 Sediment Oxygen Demand	24
5.3.3 Photosynthetic and Respiration Rates.....	25
5.4 Task 5d: Shade file (.ris).....	26
6.0 Task 6: Calibration and Validation	28
6.1 Flow	28
6.2 Water Temperature	34
6.2.1 Instabilities in temperature.....	34
6.2.2 Results.....	35
6.3 Dissolved Oxygen.....	40
7.0 Sensitivity Analysis	46
8.0 References.....	47
9.0 Appendix: Sensitivity Analysis Results.....	48
9.1 Manning Roughness.....	48
9.2 Evaporative Heat Flux Coefficients and Bed Conduction.....	50
9.3 Maximum Photosynthetic and Respiration Rate.....	53
9.4 CBOD, NBOD, and SOD	56

1.0 Introduction

The Shasta River flow, temperature, and dissolved oxygen modeling report is the second technical document that supports the development and implementation of the TVA River Management System (RMS). The RMS consists of two primary components: ADYN, a one-dimensional (vertically and depth averaged), hydrodynamic river model which produces velocities and depths for a prescribes river geometry (channel cross section and bed slope); and RQUAL, a one-dimensional water quality model that simulated temperature and dissolved oxygen for specified flow (velocity and depth from the ADYN model), biochemical oxygen demand (BOD), nitrogenous biochemical oxygen demand (NBOD), sediment oxygen demand (SOD), benthic algae photosynthesis and respiration (P and R), and meteorological conditions. The model is primarily designed to assess fate and transport of heat energy (i.e., temperature) and dissolved oxygen for specified conditions (e.g., CBOD, NBOD, SOD, P and R). The RMS does not explicitly simulate fate and transport of nutrients, the uptake of nutrients, or nutrient byproducts of benthic algae or other primary production.

This document addresses model updates relating to new geometric information (based on the 1:24 K hydrography developed by David Lamphear of the Institute for Forest and Watershed Management, Humboldt State University) and associated updates to the hydrodynamic and water quality files; the latest calibration for temperature and dissolved oxygen associated with these updates and modifications; and sensitivity analysis using the final calibrated model. These topics are presented in 7 inter-related tasks and associated subtasks – the major tasks including

- data analysis
- model selection
- geometry conversion
- re-formatting the hydrodynamic ADYN file
- formatting the water quality RQUAL files
- calibration and validation
- sensitivity analysis

Throughout this project the model effort has undergone multiple refinements and improvements. In addition to the hydrography information identified above, there has been additional water quality data available to assist in model calibration, and application of the model has provided further opportunity to interpret input data and more carefully refine model parameters. The final product is a calibrated flow, temperature, and water quality model for the Shasta River from Dwinnell Dam to the confluence with the Klamath River that forms a useful tool in assessing water quality conditions and potential impacts of modifications to flow, modifications to potential oxygen demands, and temperature control management activities. As with all numerical models of complex natural systems, responsible application of the models includes understanding and considering the limitations of both the available data and model representations when making resource management decisions.

This document is intended to supplement the technical memorandum Shasta River Modeling Status Report dated 9-13-04 (Deas and Geisler, 2004) and relies on previous work in the basin as presented in the Shasta River Flow and Temperature Modeling Project reports (Watercourse 2004a, 2004b).

1.1 Task 1. Data Analysis and Selection of Calibration/Validation Periods

The year 2002 was selected for this modeling effort based on the relatively large quantity of available flow and water temperature data. Although water quality information is limited in 2002 as compared to 2003 and 2004, there are limited flow and water temperature data in 2003 and 2004. During the 2002 field season, hourly river stage data was collected using pressure transducers at eight locations along the Shasta River (Table 1). Based on rating curves developed for each of the sites, hourly flow was calculated for these locations. Onset Hobo and Stowaway loggers were used to collect hourly temperature data at eleven sites along the river (Table 2).

Table 1. Locations of pressure transducers¹

Location	River Mile
Mouth (USGS Gage)	0.6
Anderson-Grade Road	8.0
Yreka-Ager Road	10.9
DWR Weir	15.5
Freeman Road	19.2
A12	24.1
Grenada (GID)	30.6
Louie Road	33.9

Table 2. Location of temperature loggers

Location	RM
Mouth of Shasta	0.0
Hwy 263	7.3
Anderson Grade	8.0
Yreka-Agar Rd	10.9
Hwy A-3	13.1
DWR Weir	15.5
Hwy A-12	24.1
GID	30.6
Louie Rd	33.9
Parks Creek	34.9
Shasta above Parks Creek	35.9

Meteorological data was purchased from the Western Regional Climate Center, which compiles meteorological data from Brazie Ranch. The Brazie Ranch station, which is maintained by the California Department of Forestry, is located two to 3 miles south-east

¹ Note, all the river miles have been converted to the most recent mapping (the so-called Lamphear mapping) which adds approximately 4 miles to the older mapping of 36 miles (identified in Abbott, 2002) from the mouth to the dam, for a new length of 40.6 miles.

of Yreka at latitude 41°41'07" and longitude 122° 35'39", and an elevation of approximately 3020 feet. The data from this station that were used in the RMS included hourly records of wind speed, air temperature, relative percent humidity, and solar radiation.

The periods of calibration and validation of the model were selected based on availability of flow, water temperature, and meteorological data. Flow data was particularly important. Equipment failure resulted in discontinuities in the available data. Flow data availability for all locations are outlined in Table 3. There are notable gaps in June, July, and August, but sufficient data available for model implementation.

Table 3. Available measured flow data for 2002

Start Date	Start Time	End Date	End Time	Notes
5/21/02	14:00	6/03/02	16:00	for all entries, up to 3 hours at a time may be missing from data
6/19/02	15:00	7/09/02	19:00	
8/21/02	16:00	8/31/02	14:00	
8/31/02	15:00	9/06/02	12:00	data gaps in Mouth and A12
9/16/02	15:00	10/05/02	6:00	
10/09/02	2:00	10/15/02	10:00	

Temperature data were available throughout much of the period, but certain data gaps were noted. Available periods of measured temperature data, complete at all sites for 2002 are:

- 4/18/2002 to 6/04/2002
- 7/02/2002 to 10/15/2002

Available periods of measured meteorological data for 2002 are:

- 1/01/2002 to 5/14/2002
- 6/04/2002 to 12/31/2002

Thus, the periods of full and complete flow, temperature, and meteorological measured data include:

- 8/21/2002 to 9/04/2002
- 9/16/02 to 9/30/2002
- 10/09/2002 to 10/15/2002.

Because the complete periods of measured data for temperature, flow, and meteorology were limited by the available temperature information at Louie Road, temperature for

Louie Road was estimated for the period 6/04/2002 to 10/02/2002 using an equilibrium temperature model developed by Watercourse Engineering (Watercourse, 2002). Three weeklong periods were modeled for flow and temperature, and dissolved oxygen:

- 9/17/2002 to 9/23/2002
- 7/02/2002 to 7/08/2002
- 8/29/2002 to 9/04/2002

The period from 9/17/2002 to 9/23/2002 was used for calibration of the model, and the other two periods were modeled using the same input parameters, for the purpose of validation.

Availability of water quality data was not given priority when considering the selection of modeling periods, primarily due to the paucity of available data. Characterizing flow and temperature conditions was considered of primary importance due to much greater data availability and characterizing flow and temperature is critical to representing water quality processes (due to decay rates and temperature dependence). Hourly DO data for 2002 is available, but is not continuous. The USGS collected hourly data at 4 locations: Edgewood Road (RM 47.7), Montague-Grenada Road (RM 15.57), Highway 3 (RM 13.11), and the Mouth (RM 0.6). The USFWS also collected hourly data at the mouth in 2002. Edgewood Road is located above Lake Shastina, outside of the model study area. Available dissolved oxygen data are further outlined below.

2.0 Task 2. Model Selection

The Tennessee Valley Authority's River Modeling System version 4 was selected for application to the Shasta River by Abbott (2002) and the application extended for this study. This model includes a hydrodynamic model (ADYN) and a water quality model (RQUAL). ADYN is a one-dimensional, longitudinal, unsteady flow model that simulates water-surface elevation at defined nodes along the river. The RQUAL model is also a one-dimensional, longitudinal model that simulates temperature, dissolved oxygen, CBOD, and NBOD at defined nodes along the river. RQUAL uses outputs from ADYN as well as user-input meteorology and water quality coefficients.

3.0 Task 3. Geometry Conversion

Several modifications were made during the study to update and extend the original application by Abbott (2002). The first modification was to extend the model from the confluence at Parks Creek upstream to Dwinnell Dam. Using the spatial description provided by Abbott (2002) the model was extended from RM 31.83 to 36.38. Initial testing indicated that this modification did not significantly affect model performance. The second modification was initiated when the Regional Board decided to use a different spatial description (mapping) of the Shasta River (NCRWQCB). The Lamphear hydrography was developed by the Humboldt State University's Institute for Forest and Watershed Management. The Regional Water Board suggested the Lamphear hydrography is a more detailed description of the river course than that used in previous models of the Shasta River, and that the increase in model geometry detail would allow a finer scale resolution of dissolved oxygen dynamics. The total river length determined

from the Lamphear hydrography is 4 miles longer than the previous description – providing appreciably more detail in the highly meandering reaches that run from above Hwy A-12 to the DWR weir. The entire hydrodynamic file was thus updated, along with the shade file and the water quality control file.

3.1 Task 3a: Converting to the Lamphear Hydrography for Measured Cross-sectional Geometry Locations

The ADYN hydrodynamic file requires input of cross-sectional geometry and elevation at each node in order to define the river. The additional length of the Lamphear hydrography was not uniformly distributed throughout the river from Dwinnell Dam to the confluence with the Klamath River. As such, a linear extrapolation from the previous mapping to the Lamphear hydrography was not possible. Previously measured geometry information (principally top width, depth, right bank height, and left bank height at 24 locations along the river) were identified in the Lamphear hydrography river mapping by matching the longitude and latitude and assigning the Lamphear hydrography river mile to that location (Table 4). To confirm that the Lamphear hydrography locations were consistent with approximate location of measured data, visual inspection of the old points on old river mappings and new points on new river mappings were made (Figure 1). Some points were subsequently adjusted to reflect the location of the cross-sectional measurement. For example, when the location in the original mapping was at a notable location, such as a hair-pin bend in the river, then it was placed at the hair-pin bend in the new mapping, by visual inspection. The cross-sectional geometries measured at the 24 points were then assigned to the Lamphear hydrography river mile and intermediate points were linearly interpolated between the measured data (Table 5). Any points upstream of the first measured location and downstream of the last measured location were assigned the value of the first and last, respectively. The linear interpolation was consistent with Abbott (2002) in constructing the previous input geometry.

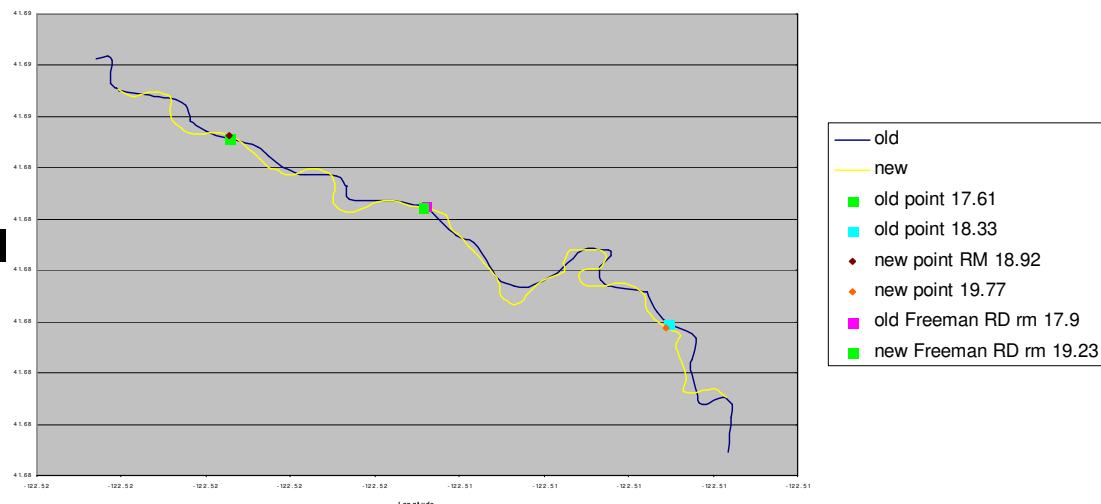


Figure 1. Comparison of old (Abbott, 2002) and new mapping from RM 18.92-19.77

Table 4. Locations of cross-sectional geometry in old (Abbott, 2002) and new river mile and longitude and latitude

Abbott's	Longitude	Latitude	Lamphear	Longitude	Latitude
2.34	-122.58880	41.80703	2.390	-122.58893	41.80704
3.14	-122.59678	41.81083	3.180	-122.59672	41.81070
3.92	-122.60814	41.80615	3.990	-122.60823	41.80618
5.50	-122.60977	41.79336	5.600	-122.61039	41.79384
6.27	-122.60195	41.78539	6.420	-122.60195	41.78545
7.07	-122.59689	41.78138	7.290	-122.59680	41.78142
7.85	-122.59271	41.77200	8.060	-122.59291	41.77195
8.56	-122.58140	41.76672	8.860	-122.58136	41.76597
9.22	-122.57933	41.75989	9.550	-122.57922	41.76000
9.93	-122.57854	41.75051	10.480	-122.57871	41.75033
10.60	-122.57117	41.74369	11.170	-122.57136	41.74368
14.72	-122.53742	41.70831	15.570	-122.53769	41.70829
15.43	-122.53141	41.70039	16.400	-122.53163	41.69973
16.19	-122.53000	41.69281	17.140	-122.52998	41.69283
16.88	-122.52908	41.68586	17.970	-122.52918	41.68587
17.61	-122.51944	41.68458	18.920	-122.51946	41.68464
18.33	-122.50904	41.68095	19.770	-122.50910	41.68087
21.95	-122.49798	41.64677	24.380	-122.49799	41.64631
22.45	-122.49552	41.64210	24.930	-122.49564	41.64239
24.97	-122.47882	41.62649	28.180	-122.47870	41.62645
25.97	-122.48253	41.61502	29.400	-122.48263	41.61502
26.47	-122.47710	41.61398	30.010	-122.47722	41.61392
26.98	-122.47343	41.60969	30.680	-122.47339	41.60974
27.95	-122.45782	41.60869	31.720	-122.45786	41.60855

3.2 Task 3b: Converting locations of estimated elevation to the Lamphear Hydrography

Elevations were converted from the original to the Lamphear hydrography using the same approach used to convert cross-sectional geometry. Abbott (2002) had taken elevation values from a USGS 1:24 K map at 26 locations. As above, locations in the Lamphear hydrography river mapping were matched by longitude and latitude and corrected, when appropriate, by visual inspection (Table 6 & Figure 2). Intermediate points were calculated using linear interpolation.

Table 5. River mile locations for bed elevations along the Shasta River

Abbott (2002) River Miles	Bed Elev. from USGS map (m)	Lamphear 2004 River Miles
0.05	620.00	0.05
0.87	630.00	0.89
1.78	640.00	1.81
2.53	650.00	2.58
3.44	660.00	3.51
4.34	670.00	4.42
4.90	680.00	4.97
5.38	690.00	5.47
6.03	700.00	6.20
6.48	710.00	6.66
7.02	720.00	7.24
8.35	730.00	8.61
11.35	740.00	11.95
12.30	745.00	13.08
14.99	750.00	15.88
16.36	755.00	17.33
19.29	760.00	20.88
21.83	765.00	24.14
25.10	770.00	28.32
30.04	780.00	33.86
32.02	790.00	36.07
32.33	795.00	36.41
33.21	800.00	37.40
34.84	810.00	39.11
35.55	820.00	39.82
36.06	830.00	40.35

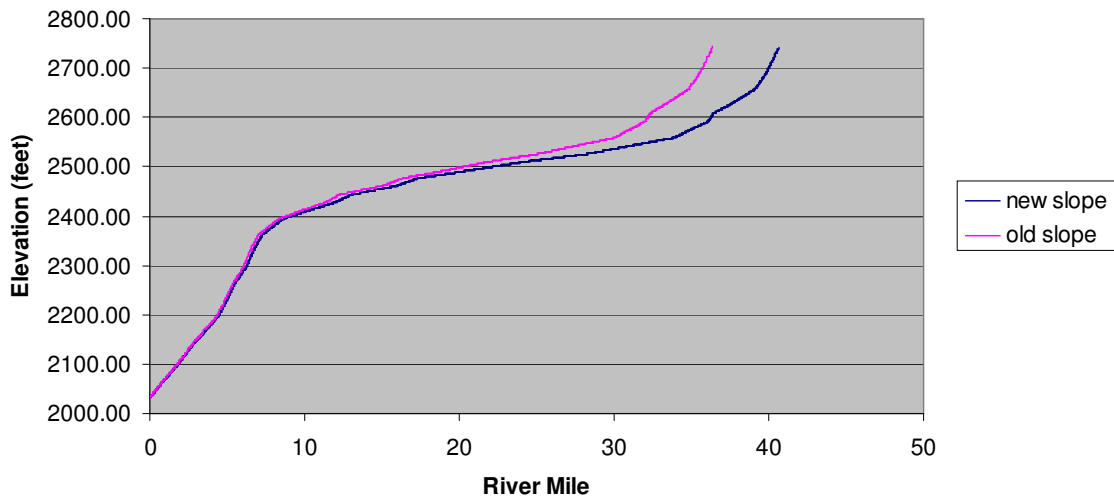


Figure 2. Shasta River slope with old (Abbott, 2002) and new geometry

3.3 Task 3c: Comparing cross-sections

The input geometry requires a cross-section at each node defined by

- a specified number of points,
- the distance of each point from the first designated point in the cross section, and
- the elevation at each point.

Cross-sections for the Lamphear hydrography were defined as in Abbott (2002). Specifically the cross-sections were assumed to be defined by five points with the third point centered from left to right bank and having the greatest depth (Figure 3). The river bank slopes (above the water surface) were assumed to be 1:1, and were extended upwards approximately 5 feet above the highest survey point to allow assessment of high flows (e.g., flows that would result in a water surface elevation above approximately 2144 ft msl in Figure 3). The channel bed and approximate river width was represented using the three interior points, with the lowest (middle) point representing a thalweg. Figure 4 shows the cross sectional area of flow and stage for a typical and a low flow condition. This “v-shaped” configuration was recommended by M. Bender (pers. comm.) to more effectively represent low flow conditions.

The elevation of the center point was taken to be the interpolated elevation calculated from the Shasta River bed elevation identified in Task 3b. The elevations of the two inner points were taken to be the bed elevation (at the center point) plus the measured depth. The elevations of the right and left banks were taken to be the two inner point elevations plus the right and left bank heights, respectively.

The Regional Board also made cross-sectional measurements in 2004. Comparisons of the Board's measured cross-sections generally showed good agreement, as indicated by the comparison of the model cross section and measured data at RM 2.77 (Figure 3). Because high flows (e.g., winter flood) were not modeled, over bank conditions were not an issue.

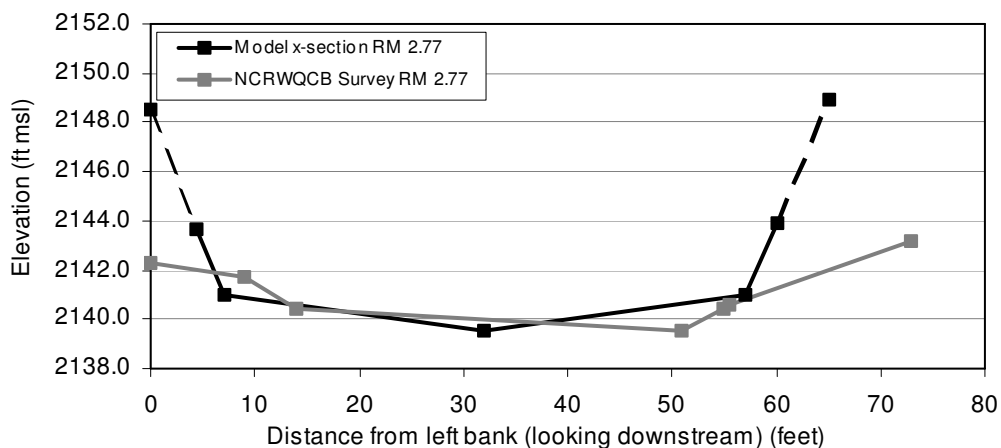
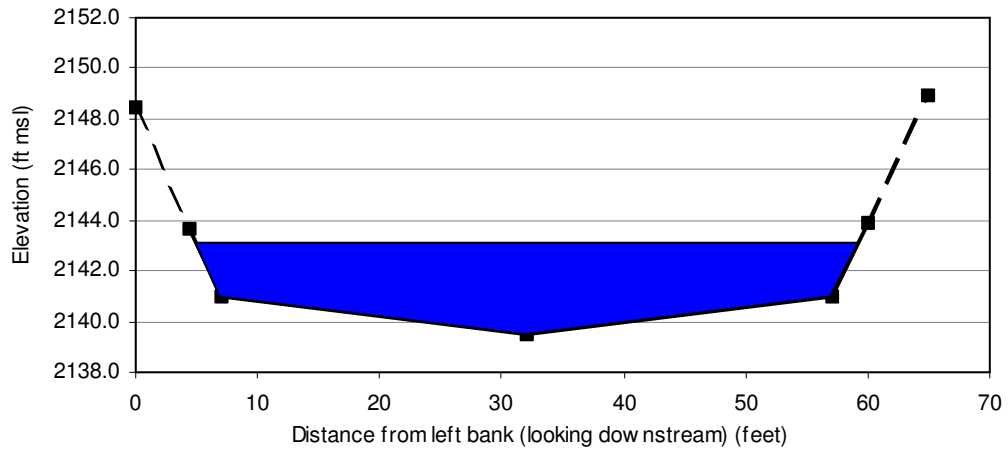
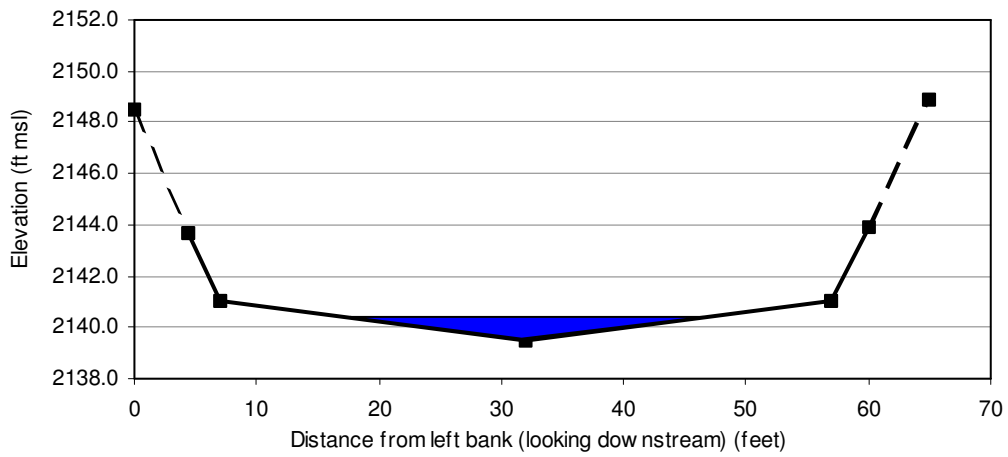


Figure 3. Sample RMS cross-section representation at RM 2.77 and measured cross section



(a)



(b)

Figure 4. Cross sectional flow area and stage for (a) typical and (b) low flow conditions for representative cross -section

3.4 Task 3d: Updating Model Node Locations in the Lamphear Hydrography

Information was available at increments of 0.01 miles in the Lamphear hydrography. This translates to 4168 points describing the river from Dwinnell Dam to the confluence with the Klamath River. In the previous model (Abbott, 2002) 438 nodes were used to describe the river. One limitation of the River Modeling System hydrodynamic model is that maximum number of nodes is 999. Thus, the total number of available points in the Lamphear hydrography had to be reduced by approximately one-quarter without losing significant overall river length. To minimize impact on river length, nodes were primarily removed from the straighter portions of the river, as shown in Figures 6 & Figure 7. Distance between nodes was never greater than seven times the distance between previous or subsequent pairs of nodes, in order to aid the ADYN numerical calculations. The final modeled river length was 39.05 miles, a reduction of 1.57 miles, or 3.9 %.

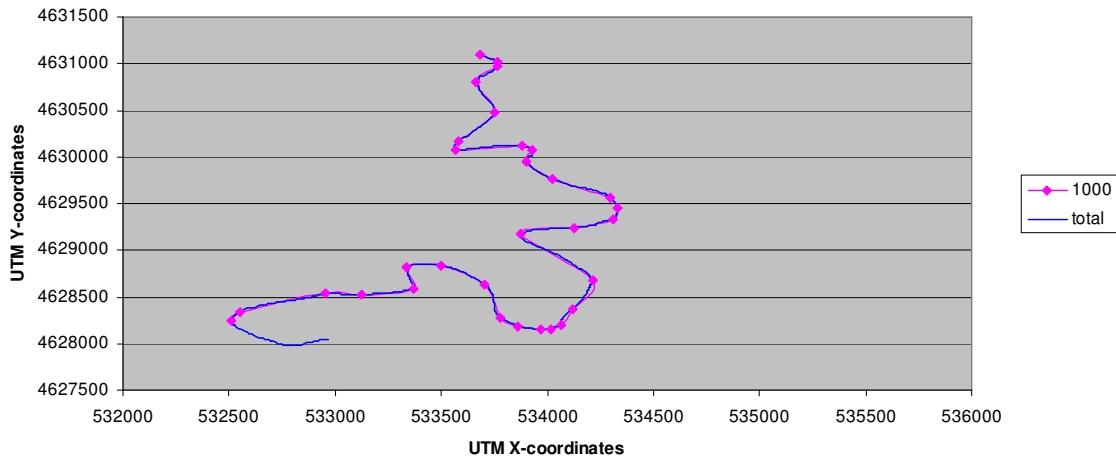


Figure 5. Nodes assigned to RM 0-5

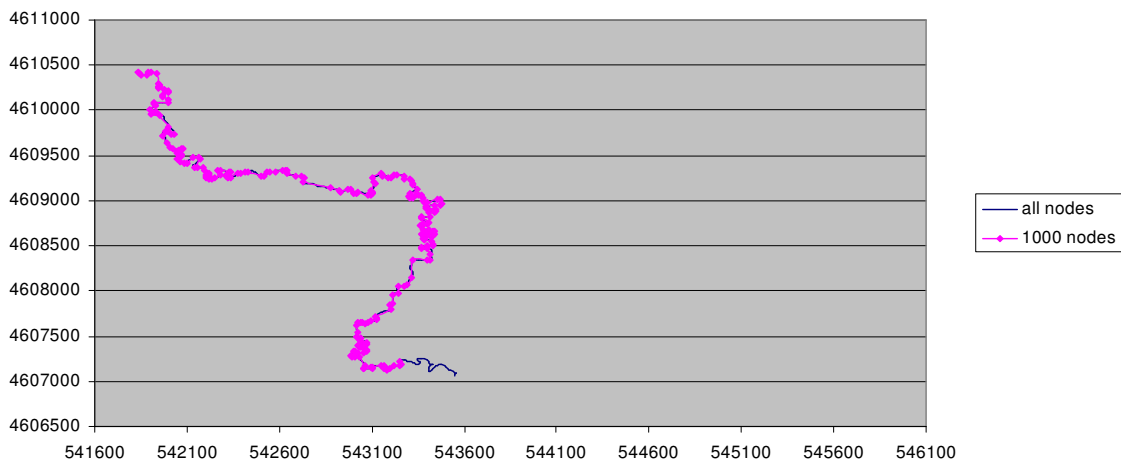


Figure 6. Nodes assigned to RM 25-30

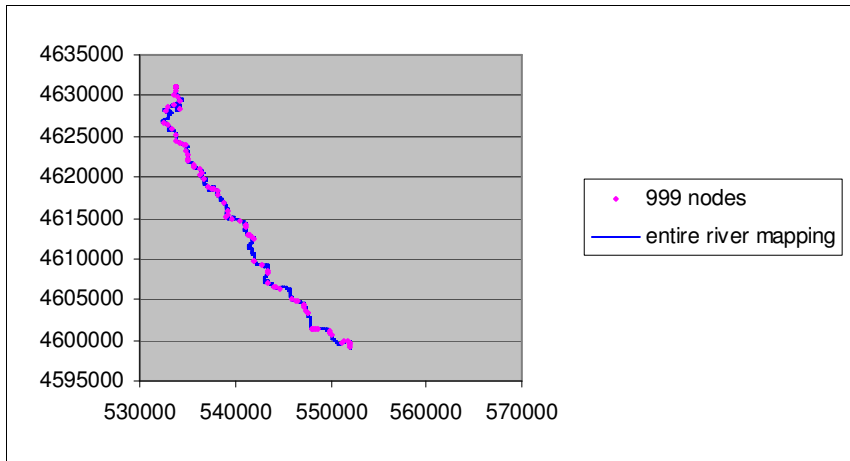


Figure 7. 999 nodes mapped along river

3.5 Task 3e: Calculating new river azimuths

New azimuths between model nodes representing the orientation of the river as it traverses the region from Dwinnell Dam to the confluence with the Klamath River were also calculated for the new river geometry. The method applied for calculating azimuths (in radians based on zero degrees being north) from longitude and latitude was:

$$dy = lat_2 - lat_1$$

$$dx = long_2 - long_1$$

$$\text{if } dx > 0, \text{ then radians from north} = \Pi/2 - \text{atan}(dy/dx)$$

$$\text{otherwise, radians from north} = 3\Pi/2 - \text{atan}(dy/dx)$$

where lat_1 , $long_1$ and lat_2 , $long_2$ refer to the latitude and longitude of adjacent model nodes.

3.6 Task 3f: Converting shading file

Riparian vegetation shading is represented in the model using various attributes, including tree height and solar radiation transmittance. These shade attributes are assigned for each node and can vary for the left and right river banks. Solar radiation transmittance is defined as the amount of solar radiation that passes through the tree canopy and reaches the water surface. A value of 1.0 represents no shade, a value of 0.0 would represent complete shade.

To transform the original shade file to the Lamphear hydrography, the percentage of total river length for each nodal interval was calculated for the original and new mapping and the transmittance was re-mapped by matching the transmittance value at the original percentage of total length to the same percentage of total length in the new mapping. The original shading file was also altered to limit transmittance of solar radiation to 50 percent, by a simple linear mapping. This was based on additional information on riparian transmittance. Lowney (2000) provides a discussion of riparian transmittance:

“Most of the solar radiation reaching the canopy is absorbed, the remainder is either

reflected (scattered backward) or transmitted (scattered forward) towards the water surface. Monteith and Unsworth (1990) suggest that for a deep canopy of foliage, leaves absorb approximately 80 percent of incident radiation, reflect 10 percent, and transmit 10 percent. Attenuation of solar radiation by the forest canopy decays exponentially, strongly dependent on the leaf area index (LAI) – the plan area of leaves per unit ground area, and an extinction coefficient that characterizes orientation of individual leaves. Forest canopies are generally more efficient in absorbing solar radiation than other vegetative surfaces due to their increased surface irregularity and canopy density. Moreover, it is reasonable to assume that a well established riparian forest, particularly a diverse community will absorb more solar radiation than a single row of trees.”

Lowney also identified an assumed transmittance rate, based on field measurements, of approximately 10 percent for full riparian forests, but higher values– between 15 and 25 percent – for riparian bands and strips. These values are consistent with Abbott (2002) for fully shaded reaches. However, additional discussions with Lowney (C. Lowney, pers. comm.) and others (Watercourse, 2002b) indicate that transmittance rates may be larger due to variability in the existence of woody riparian vegetation, incomplete tree canopy, the distance the trees are from the bank, relative health of the riparian vegetation, and other factors. Thus, maximum transmittance was set to 50 percent for calibration as a conservative estimate. Certain scenarios and applications may examine higher rates of solar radiation attenuation assuming high quality riparian vegetation conditions.

The shading file (.ris), constructed by Abbott (2002) was initially extended to Dwinnell Reservoir by assigning the shading input at the highest previous point (approximately Parks Creek at RM 31.83 in original geometry) to all upstream nodes up to Dwinnell Dam (RM 36.38 in original geometry). This assumption was maintained when the original geometry was mapped to the Lamphear hydrography, i.e., shading was maintained constant from approximately Parks Creek up to Dwinnell Dam – an assumption that is supported by both Deas et al (1997) and CWRCB (2005). Abbott (2002) provides detailed descriptions of the shading logic, input files, and other information.

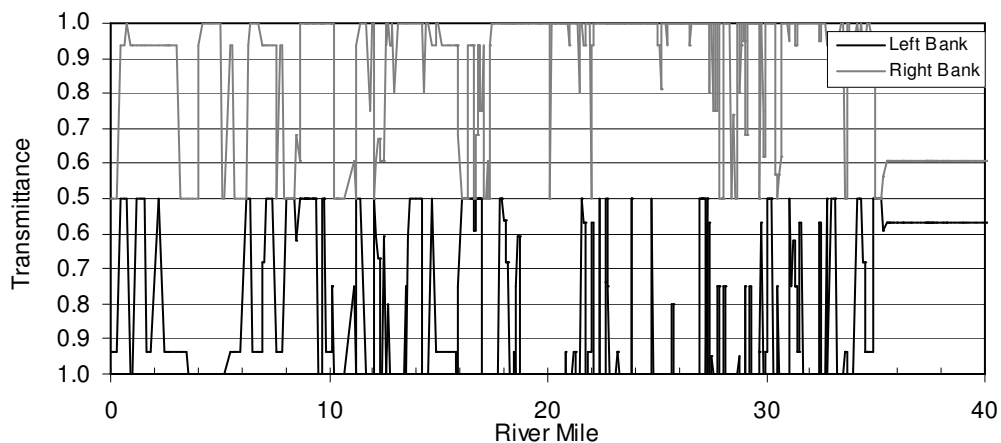


Figure 8. Longitudinal distribution of shade conditions on the Shasta River (tree height assumed 22 feet where present)

4.0 Task 4: Re-formatting the Hydrodynamic ADYN file

The TVA hydrodynamic model (ADYN) requires input of river geometry, boundary conditions for flow, and initial conditions for flow. The updated geometry was input as described above; however, the upstream inflow to the model domain as well as tributaries and other inputs and outputs was required.

The river was modeled as a single reach with 11 lateral inputs (or outflows). To develop the flow boundary conditions, the river was divided into sub-reaches based on the locations of flow measurement, major diversions, and tributaries. Major diversions and tributaries were modeled as point sources and the rest of the river was represented as sub-reaches with distributed accretions or depletions. The accretions/depletions were calculated using a water balance based on daily averages of measured flows over the reach:

$$(\text{daily average flow at } x_i) - (\text{daily average flow at } x_{i+1}) = \text{accretion (+) or depletion (-)}$$

where x_i represents the upstream end of the reach and x_{i+1} is the downstream end of the reach.

Where major diversions or tributaries with known flows fall within the reach, i.e., between locations x_i and x_{i+1} , they are included as point sources or sinks in the calculation of accretions and depletions:

$$(\text{daily average flow at } x_i) - (\text{daily average flow at } x_{i+1}) - \text{spring inflow} + \text{diversion} = \text{accretion (+) or depletion (-)}$$

These accretions and depletions are entered for all days in the simulation. This approach is useful when manipulating specific sub-reaches, as in increasing flows in a single sub-reach or modifying water quality in a particular sub-reach. The various tributaries, diversions, and accretion/depletions are outlined in Table 6.

Initial conditions were developed by running the model with identical daily boundary conditions for 8 days to create a steady state condition. This steady streamflow condition forms the initial conditions for model simulations, and are presented in Task 6.

5.0 Task 5: Formatting the Water Quality RQUAL files

5.1 Task 5a: Boundary condition file (*.rib)

Boundary conditions for RQUAL consist of a headwater condition, point inputs, and distributed inputs. Generally, temperature and DO data vary hourly, while CBOD, and NBOD are maintained constant. The locations, river mile, and boundary condition type are shown in Table 6. Hwy A-12 and DWR weir are included as benchmarks.

Table 6. Hydrodynamic input locations and types

Name	Abbreviation	River Mile	Boundary Condition Type
Dwinnell Dam	DWIN	40.62	Headwater
Riverside Drive	RIV	39.94	Point
Parks Creek	PKS	34.94	Point
Big Springs	BIGS	33.71	Point
Grenada Irrigation District (GID)	GID	30.59	Diversion
GID to Hwy A-12	G-A12	27.35	Distributed
	A12*	24.11	n/a
Hwy A-12 to Freeman Lane	A-SRF	21.60	Distributed
Shasta Water Users Association	SWUA	17.85	Diversion
Freeman Lane to DWR Weir	S-DWR	17.32	Distributed
	DWR*	15.52	n/a
DWR Weir to Yreka Ager Rd	DWR-Y	13.26	Distributed
Yreka Ager Rd to Anderson Grade	Y-AND	9.58	Distributed
Yreka Creek	YREKA	7.88	Point

* These boundary condition locations are included in the model input files for testing, but not used in the calibration or production simulations

5.1.1 Temperature

The water quality component of the TVA model (RQUAL) uses the heat budget approach that quantifies pertinent factors by formulations based on physical processes.

The heat budget approach quantifies the net exchange of heat at the air-water interface.

TVA has extended the approach to also include heat exchange at the water-bed interface.

This net change may be expressed as the sum of the major sources and sinks of thermal energy or the sum of the heat fluxes.

TVA Heat Budget Formulation

$$Q_n = \frac{Q_{ns} + Q_{na} + Q_{bed} - Q_b - Q_e - Q_c}{D}$$

where:

Q_n = the net heat flux (representing the rate of heat released from or added to storage in a particular volume) (kcal/m³s)

Q_{ns} = net solar (short-wave) radiation flux adjusted for shade (kcal/m²s)

Q_{na} = net atmospheric (long-wave) radiation flux (kcal/m²s)

Q_{bed} = net flux of heat at the water- channel bed interface (kcal/m²s)

Q_b = net flux of back (long-wave) radiation from water surface (kcal/m²s)

Q_e = evaporative (latent or convective) heat flux (kcal/m²s)

Q_c = conductive (sensible) heat flux (kcal/m²s)

D = mean depth (m).

For a more complete discussion of the heat budget terms, the reader is referred to Abbott (2002).

In addition to heat exchange at the air-water and bed-water interface, heat energy can enter and leave the river system via inputs (e.g., tributaries) and outputs (e.g., diversions).

Temperature boundary conditions can be entered for both point sources and distributed sources. For the point sources, values are input at the designated river mile. For the distributed sources, temperature values are input over the same reach as the distributed flow is applied. Outflows are assumed to leave the river at the temperature of the river at the identified location.

Because available temperature measurements at Parks Creek and Shasta above Parks were limited, hourly temperature measurements at Louie Road were used as input for the upstream boundary condition (Dwinnell Dam), Riverside Drive, and Parks Creek. Temperature was input for each hour of the simulation.

Absent water temperature data from Big Springs Creek, several water temperatures data sets were explored. Initially data from the Shasta River at Grenada Irrigation District was applied after Abbott (2002). However, review of this temperature signal indicated that the diurnal phase was lagged, peaking late in the evening, compared with other locations on the river. Sensitivity testing with the model indicated that this lag may have been associated with impoundment of the river at the GID diversion. Subsequently, data from the Shasta River at Hwy A-12 were applied as the boundary condition at Big Spring Creek because there was not a lag at Highway A-12. Further investigation of Regional Board data indicated that the lag in diurnal temperatures occurs above the GID impoundment (Figure 9), suggesting that the springs complex associated with Big Springs or other springs, and possibly water resources development (e.g., irrigation schedules and operations) lead to this signal. Thus, temperatures from GID were ultimately used as the boundary conditions at Big Spring Creek. Because there is a lack of site specific data for Big Springs Creek (for flow, water temperature and other parameters) it is important to consider this boundary condition when assessing alternatives that alter Big Springs inflow temperature.

Temperatures for all accretions between GID and Anderson Grade were assigned the temperature at Anderson Grade. This decision was based on review of temperature data from 2001 and 2002 which indicated that temperatures were approaching equilibrium temperature by the end of the Shasta Valley (i.e., near Anderson Grade). Lacking any time series data for return flows, it was assumed that irrigation return flows would be near equilibrium temperature, and thus Anderson Grade time series data was used as a surrogate. Temperature boundary conditions are shown in Figure 10.

5.1.2 Dissolved Oxygen, NBOD, CBOD

Dissolved oxygen, carbonaceous biochemical oxygen demand (CBOD), and nitrogenous biochemical oxygen demand (NBOD) are represented in the RQUAL model. The time varying representation of dissolved oxygen is represented as

$$\Sigma[\partial O/\partial t] = K_2(O_s - O) - K_d L - K_n N + (P - R - S)/D$$

Where

t = time (s)

O = dissolve oxygen concentration (mg/l)

O_s = saturation dissolve oxygen concentration (mg/l) (based on elevation and water temperature (See TVA, 2001))

K_2 = reaeration rate based on one of several methods (see TVA, 2001), temperature corrected (1/s)

K_d = CBOD deoxygenation rate, temperature corrected (1/s)

L = CBOD concentration (mg/l)

K_n = NBOD deoxygenation rate, temperature corrected (1/s)

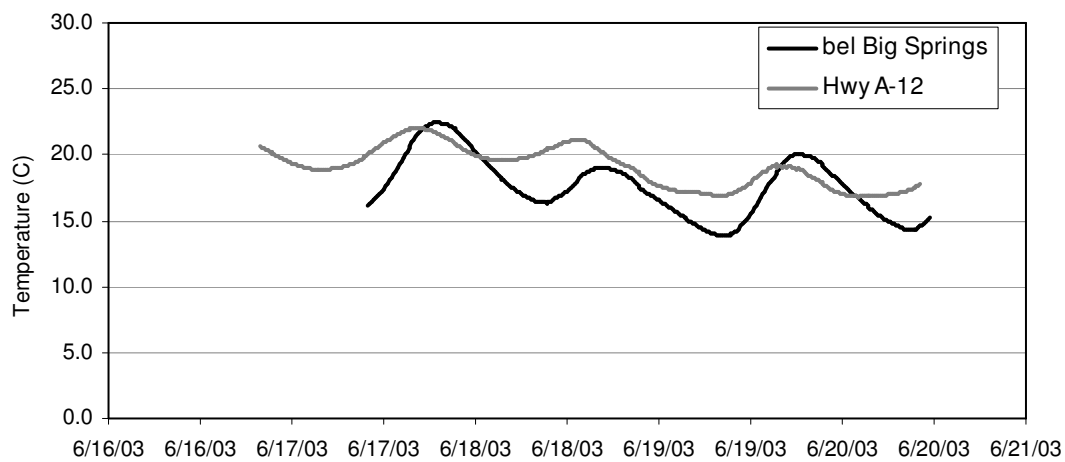
N = NBOD concentration (mg/l)

P = Photosynthetic rate of macrophytes ($gO_2/m^2/s$)

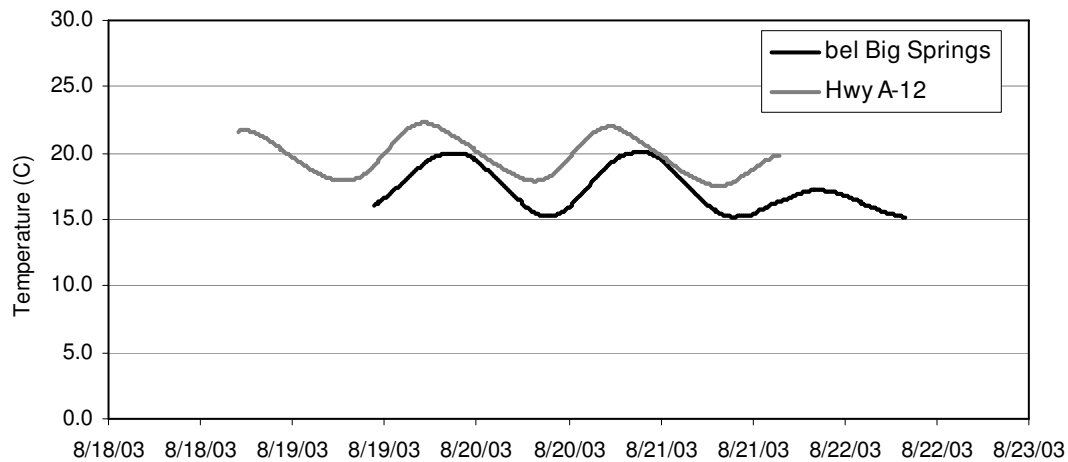
R = Respiration rate of macrophytes ($gO_2/m^2/s$)

S = Sediment oxygen demand ($gO_2/m^2/s$)

D = mean depth (m)

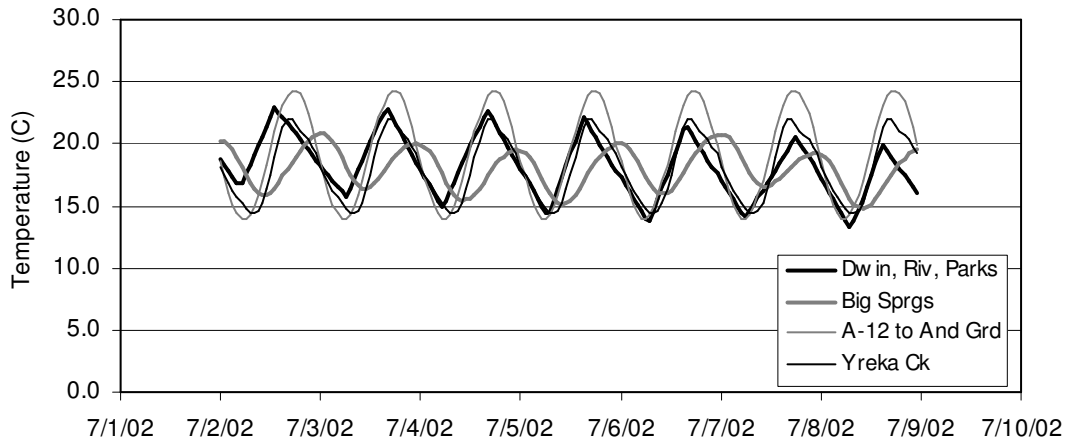


(a)

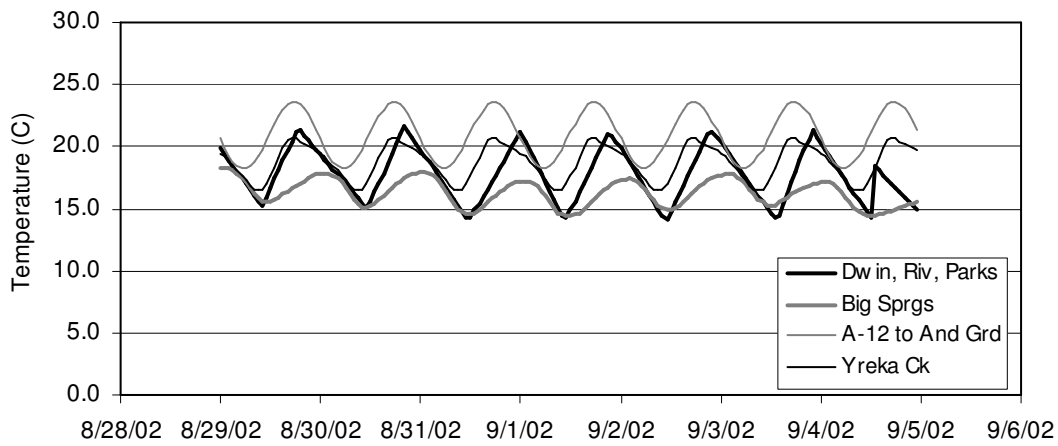


(b)

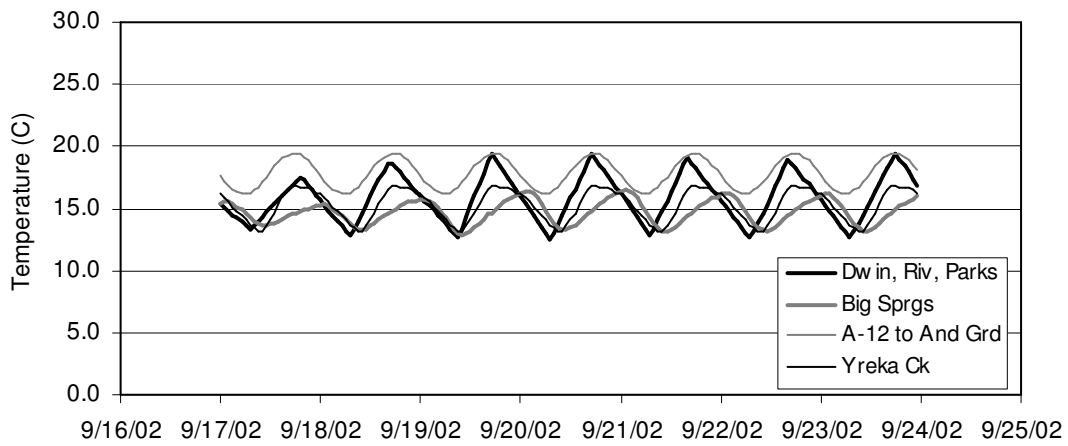
Figure 9. Observed water temperature for the Shasta River at Highway A-12 and below Big Springs Creek (CRWQCB, 2004)



(a)



(b)



(c)

Figure 10. Water temperature boundary conditions for the July, August-September, and September calibration periods

CBOD and NBOD are both represented as first order decay:

$$\Sigma[\partial L/\partial t] = -(K_d+K_s)/L$$

and

$$\Sigma[\partial N/\partial t] = -K_n N$$

Where

K_s = CBOD settling rate (no oxygen demand exerted) (1/s)
and t , L , N , K_d , K_n are defined previously.

Note, the units of time represented in the above equation may differ from the model required input values. For example, although all temporal units identified above are represented in seconds, model input decay rates are 1/day.

Sediment oxygen demand and macrophyte photosynthesis and respiration are discussed separately under initial conditions and water quality coefficients, below, because they are specified by the user and are not simulated state variables.

Dissolved oxygen, CBOD, and NBOD boundary conditions were applied at the same locations as temperature.

Dissolved Oxygen

Dissolved oxygen data was unavailable at all boundary conditions for the calibration and validation periods. Thus, all DO boundary conditions were estimated using saturation concentration based on water temperature and atmospheric pressure (based on the elevation of the Shasta Valley):

$$\text{saturated DO (mg/L)} = \exp((-139.34411) + (1.575701 \times 10^5 / T) - (6.642308 \times 10^7 / T^2) + (1.2438 \times 10^{10} / T^3) - (8.621949 \times 10^{11} / T^4))$$

where water temperature, T , is in degrees Kelvin. Boundary conditions are represented graphically in Figure 11.

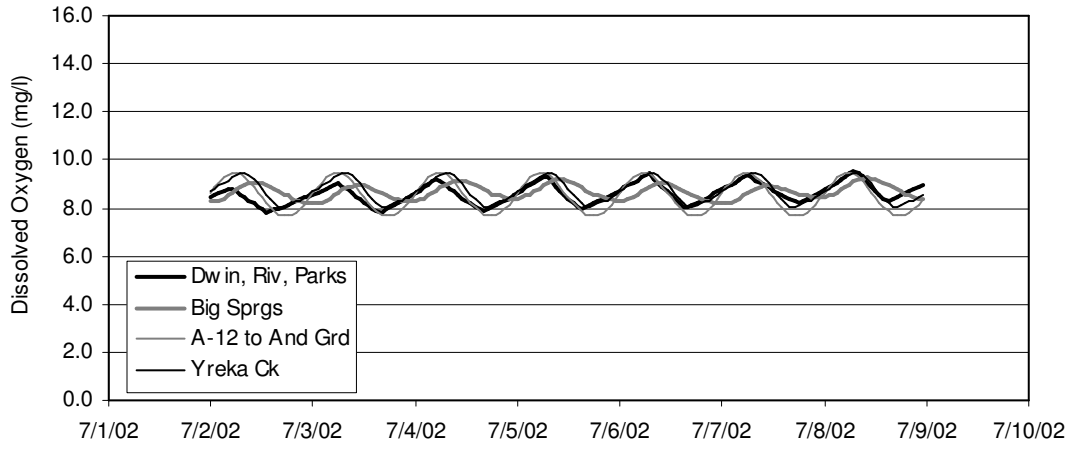
CBOD

Based on NCRWQCB data CBOD boundary conditions were generally non-detect (less than 2 mg/L). There were 3 values of $CBOD_5$ above the detection limit: 3.5 mg/L at Yreka-Ager Road on August 19, 2003, 3.4 mg/L at Riverside Drive on August 19, 2003, and 15.0 at Riverside Drive on August 20, 2003. Boundary conditions were estimated at 3.5 mg/L because all boundary condition locations either lacked data or were below the assumed detection limit. The model requires $CBOD_u$, and Hauser (2002) notes that $CBOD_u$ is usually 1.5 to 3 times $CBOD_5$. $CBOD_u$ was assumed equal to 5 mg/l for this application for all boundary conditions for all simulation periods.

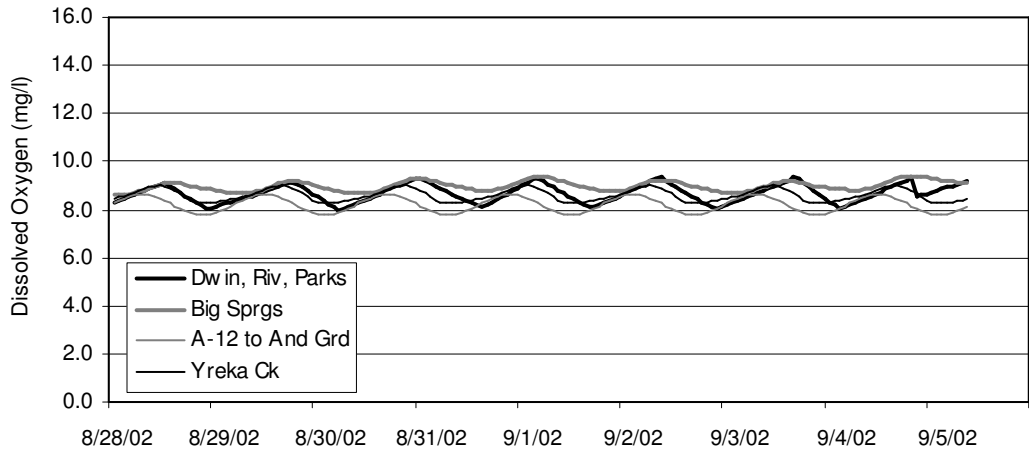
NBOD

There was appreciably more nitrogen information to estimate NBOD boundary conditions. Chapra (1997) estimates NBOD based on total Kjeldahl nitrogen (TKN):

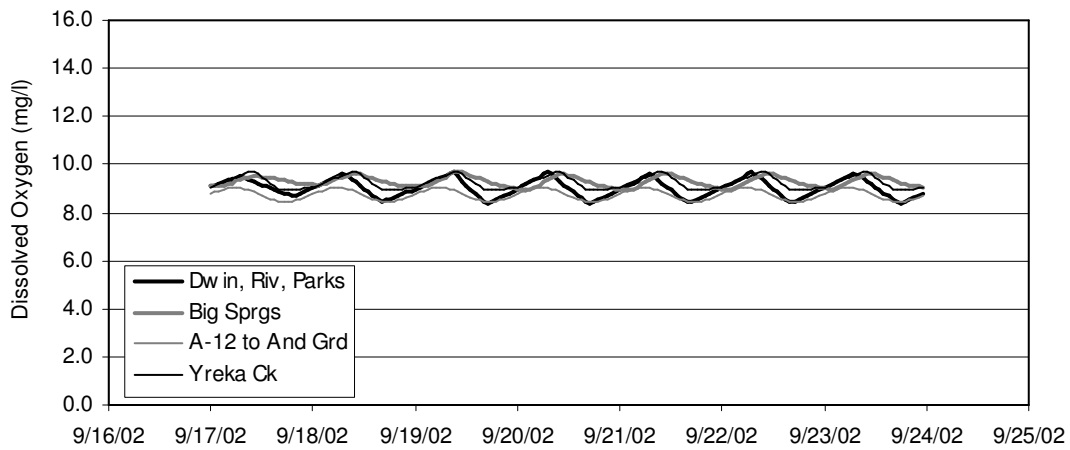
$$NBOD \text{ (mg/L)} = 4.57 * TKN \text{ (mgN/L)}$$



(a)



(b)



(c)

Figure 11. Dissolved oxygen boundary conditions for the July, August-September, and September calibration periods

The boundary conditions for NBOD were based on TKN values (Table 7). The NBOD values used for boundary conditions were 2.74 mg/l for Dwinnell Dam, Riverside Drive and Parks Creek; 0.91 mg/l for Big Springs Creek; 5.53 mg/l for accretions between Highway A-12 and Anderson Grade (based on limited tailwater return flows data), and 1.33 mg/l for Yreka Creek (Figure 12).

Table 7. Available CBOD and TKN data

Location	Metric	BOD ₅ (mg/L)	TKN (mg N/L)
Dwinnell Dam ^a	Minimum	ND	ND
	Maximum	15.0	1.2
	Average	5.35	0.57
	Median	2.45	0.60
	Count	4	39
Big Springs ^b	Minimum	ND	ND
	Maximum	ND	ND
	Average	NA	NA
	Median	NA	NA
	Count	3	3
Tailwater Return Flow / Distributed Flow ^c	Minimum	1.5	0.3
	Maximum	7.0	3.9
	Average	2.7	1.2
	Median	2.0	0.9
	Count	11	15
Yreka Creek ^d	Minimum	ND	ND
	Maximum	ND	0.75
	Average	NA	0.29
	Median	NA	0.20
	Count	2	28

ND = Non Detect

NA = Not Applicable

^a Dwinnell Dam outflow data collected from 1995 through 2003 by CRWQCB and DWR at Riverside Drive.

^b Big Springs data collected in 2003 at Big Springs Lake outflow by CRWQCB.

^c Tailwater return flow data collected in 2003 by CRWQCB.

^d Yreka Creek data collected from 1999 through April 2005 by City of Yreka, CRWQCB, and DWR at Anderson Grade Road and Nursery Bridge.

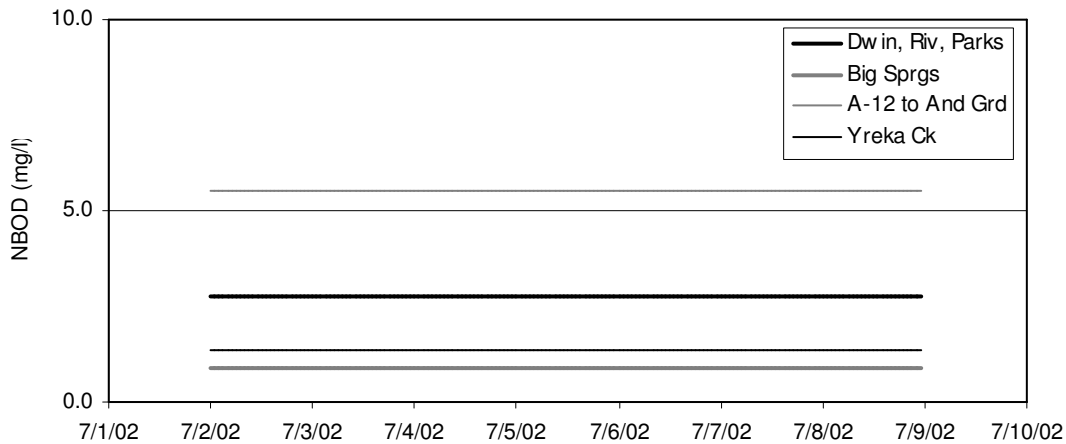


Figure 12. NBOD boundary conditions for the July, August-September, and September calibration periods (same for all periods, only July presented)

5.2 Task 5b: Meteorology file (*.rim)

The meteorology input requires cloud cover, dry bulb temperature, dew point temperature, barometric pressure, wind speed, and short wave solar radiation. The raw data from Brazie Ranch provided dry bulb temperature, wind speed, solar radiation, and relative humidity for the calculation of dew point temperature. Dew point temperature was calculated after Chapra (1997) as:

$$\text{DPT (C)} = 237.3B/(1-B)$$

where

$$B = \ln(e/6.108)/17.27$$

$$e = \text{vapor pressure (mb)} = \text{RH} * e_s / 100$$

where

$$\text{RH} = \text{relative humidity (\%)}$$

$$e_s = \text{saturation vapor pressure (mb)} = e_s = 6.108 \exp[17.27T/(T+237.3)]$$

$$T = \text{Air temp (C)}$$

Cloud cover was set to zero for the modeled periods, which is a typical condition for late spring through early fall periods. Barometric pressure was estimated based on local elevation to be constant at 930.41mb.

5.3 Task 5c: Water quality coefficients and initial conditions file (*.ric)

The model requires a wide range of water quality coefficients as well as initial conditions, e.g., numerical solution scheme for RQUAL; initial conditions for temperature, DO, CBOD, and NBOD; water quality coefficients and rate constants; and river azimuths. Outlined herein are final model parameter and coefficient values, specification of sediment oxygen demand rates (CRWRCB, 2004c), determination of maximum photosynthetic and respiration rates (CRWRCB, 2005) associated with primary production, and initial conditions. Initial conditions are constant for the entire river. Model results for the first day or so should be discarded because they retain the characteristics of the initial conditions.

5.3.1 Rates, Constants, Coefficients and Other Model Parameters

Pertinent model input parameter names, description, value, and pertinent notes are presented in Table 8.

Table 8. Input parameters for .ric file

Coefficient	Description	Value	Notes & Reference
PRT	print interval for standard output file (hrs)	1.0	hours
IPLT	flag to create plot file	1	1 = yes
THET	spatial derivative weighting factor for 4-point implicit scheme	0.55	range is 0.5-0.6. (p. 114 of User Guide)
TSI	model testing coefficient	1.0	recommended value p. 97 of User Guide
PLT	plot file interval (hrs)	1.0	
NSCH	numerical solution scheme	H	Holly-Priessman scheme for shallow or deep water
PDC	Holly-Priessman numerical scheme limit on C	0.01	recommended by User Guide for stability
PDCX	Holly-Priessman numerical scheme limit on dC/dx	-1	recommended by User Guide for stability
IRS	flag for shading file Abbott (2002)	1	1 = include shading
PHI	latitude of river (decimal degrees)	41.875	Abbott (2002) p. 68
ALON	longitude of river (decimal degrees)	122.630	Abbott (2002) p. 68
TFOG	time of morning fog lift	6.00	Abbott (2002) p. 68
BW	bank width (ft) from river edge to barrier at above river mile	0.0	Abbott (2002) p. 155
AA	coefficient in wind speed function ($m^3/mb/s$) for evaporative cooling ($\psi = aa + bb*wind$)	1.0E-9	Calibrated value range = 0E-9 to 4E-9 p. 102 of User Guide
BB	coefficient in wind speed function (m^2/mb) for evaporative cooling ($\psi = aa + bb*wind$)	1.5E-9	Calibrated value range = 1E-9 to 3E-9 p. 102 of User Guide
XL	effective channel bed thickness of upper layer for bed heat conduction (cm)	10	recommended value p. 102 of User Guide
XL2	effective channel bed thickness of deep layer (cm)	50	recommended value p. 102 of User Guide
DIF	thermal diffusivity of bed material (cm^2/hr)	27.7	recommended value and chosen based on calibration. (range 25 to 50)
CV	bed heat storage capacity ($cal/cm^3^{\circ}C$)	0.68	recommended value p. 102 of User Guide
BETW	fraction of solar radiation absorbed in surface 0.6 m of water	0.4	recommended value p. 102 of User Guide
BEDALB	albedo of bed material	0.25	recommended value p. 103 of User Guide
SHDBT	fraction of drybulb/dewpoint depression by which dry bulb is cooler over shaded water	0.5	recommended value p. 103 of User Guide
THR	temperature correction coefficient for reaeration	1.024	Chapra (1997) p.41, User Guide p. 104
THB	temperature correction coefficient for CBOD decay	1.047	Chapra (1997) p.41, User Guide p. 104
BK20	deoxygenation rate at 20°C for CBOD (1/day)	0.2	Chapra (1997) p. 357-358
THN	temperature correction coefficient for NBOD decay	1.09	User Guide p. 104
NK20	deoxygenation rate at 20°C for NBOD (1/day)	0.2	Chapra (1997) p. 424-425 RANGE 0.1-0.5 day^{-1} . For shallow streams, can be > 1
THS	temperature correction coefficient for SOD	1.065	user guide p. 104 Chapra (1997) p.41 gives 1.08,
EXCO	light extinction coefficient (1/m)	0.1	range 0.05-0.3; 0.05 clean water; 0.3 turbid water; (user's guide p.104).
HMAC	average weed height from bottom of channel (ft)	1.0	range of weed height 1-3 feet (User Guide, p. 104)
THPR	temperature correction coefficient for macrophyte photosynthesis and respiration	1.08	user guide p. 104
IK2E	flag for reaeration equation choice	3	see p. 104 User Guide. Owens formulation was chosen because it was developed for shallow rivers.
BS20	CBOD settling rate (1/day)	0.656	Calculated as $K_s = v_s/depth$ assume $v_s = 0.3$ m/d (Chapra (1997) p. 358 provides a range of 0.1-0.5 m/d). Avg depth of river : 1.5 ft

Table 8 (cont.) Input parameters for .ric file

Coefficient	Description	Value	Notes & Reference
SFAC	factor to multiply all SK20 in reach to test sensitivity	1.0	p.108 User Guide
PFAC	factor to multiply all PMAX20 in reach to test sensitivity	1.0	p.109 User Guide
PMAX20	photosynthetic rate for attached algae (gO ₂ /m ² /hour)	See below	See below
RFAC	factor to multiply all RESP20 in reach to test sensitivity	1.0	p.110 User Guide
RESP20	attached algae respiration rate (gO ₂ /m ² /hour)	See below	See below

User Guide refers to Hauser, G.E. and G.A. Schohl, 2002

5.3.2 Sediment Oxygen Demand

To represent the spatial variability in sediments that may yield oxygen demand, the sediment oxygen demand rate at 20°C (SK20) was based on USGS (2004) studies and qualitative field mapping of sediments completed by the North Coast Regional Water Quality Control Board. The results are provided in Table 9. These rates are temperature corrected in RQUAL.

Table 9. Spatial Distribution of sediment oxygen demand (input parameter SK20)

River Mile	SOD rate (gO₂/m²/day)
40.62	0.2
39.94	0.2
38.65	0.5
32.03	0.5
30.65	2.0
27.50	0.2
25.79	0.1
24.10	0.1
19.11	0.1
17.78	2.0
15.40	1.5
14.68	1.5
13.74	1.5
13.16	2.0
12.50	0.2
11.10	0.2
10.69	0.2
8.65	0.2
6.42	0.1
1.05	0.1
0.72	0.1
0.00	0.1

Based on field work and qualitative distribution of sediments completed by the North Coast Regional Water Quality Board

5.3.3 Photosynthetic and Respiration Rates

Extensive sampling and observation of the types and quantities of attached algae and macrophytes in the Shasta River were undertaken in 2004 by the CRWQCB (2005). However, light and dark bottle tests were not performed, so explicit values for photosynthetic rate were not available. The qualitative information provided by the NCRWQCB (Table 10) provided a mapping of rates along the river based on the following algal densities:

- 0-10% low coverage
- 11-60% medium coverage
- 61-100% high coverage

Table 10. Qualitative reach description of benthic algae cover and relative coverage

Reach (NCRWQCB descriptor)	% Benthic Cover	River Mile		Relative Coverage
		From	To	
Riverside	35	39.27	40.47	med
Hidden Valley	75	32.06	39.27	high
E. Louie Road	70	30.57	32.06	high
u/s GID	85	25.85	30.57	high
d/s GID	40	24.11	25.85	med
15 - u/s A12	10	22.14	24.11	low
14 - A12 to DeSoza	15	16.08	22.14	med
De Soza to Brecada	70	14.74	16.08	high
Brecada to u/s Big Bend	10	13.8	14.74	low
Big Bend	90	13.31	13.8	high
d/s Big Bend to u/s Hwy3	30	12.63	13.31	med
u/s Hwy3 to impoundment	70	12.24	12.63	high
d/s impoundment - short reach	20	11.73	12.24	med
d/s impoundment to Y-A Rd	15	10.9	11.73	med
Y-A Rd to riparian	95	10.56	10.9	high
riparian to 263	50	6.36	10.56	med
263 to d/s Pioneer Bridge	5	4.23	6.36	low
d/s Pioneer Bridge to u/s gage	25	4.05	4.23	med
gage to mouth	5	0	4.05	low

Mapping the Results to the Algae Study

Maximum photosynthesis rates, P_{max} , for each section of the river were derived from calibration. Photosynthesis by most freshwater benthic algae is a non-linear function of light intensity. At low irradiances, photosynthetic rate increases linearly with increasing light, and appears to be limited primarily by the number of photons captured by photosynthetic pigments. At mid-level irradiances, photosynthesis begins to level off as light becomes saturating. The maximum rate of photosynthesis, whether reached asymptotically (no photoinhibition) or as a peak (photoinhibition), is referred to as P_{max} .

Three sites, representing the three levels of relative coverage, were chosen primarily on the basis of available dissolved oxygen observations. These sites included Shasta near

Mouth, Shasta at Hwy3, and DWR Weir, representing low, medium, and high levels of observe coverage. During calibration, P_{max} was adjusted to best fit available data at each site. For simplicity, only one value of P_{max} was derived for each of the three sites. The sites and derived values of P_{max} are presented in Table 11.

Table 11. Calibrated P_{max} values

Location	RMI	Calibrated (g O ₂ /m ² /hour)
DWR	15.52	3.15
Hwy3	13.2	2.36
Mouth	0.66	1.20

These calibrated values of P_{max} were then applied to the entire river according to the distribution of benthic algae coverage observed by NCRWQCB. This distribution is presented in Table 12 and shown in Figure 13 in the following section.

RQUAL model does not explicitly model algal growth. Rather the user specifies standing crop that can vary in space and per simulation period (e.g., the standing crop can vary among the July, August, and September period). Respiration was assumed to equal 20 percent of P_{max} for July and August when standing crop is close to the seasonal high. However, for late September, the respiration was reduced by 50 percent to represent a smaller standing crop in the fall period. P_{max} and respiration (at 20°C, RQUAL corrects for temperature) inputs for each of the three periods simulated are provided in Table 13, below.

5.4 Task 5d: Shade file (.ris)

The shade file is an addition to the RQUAL program (Abbott, 2002). It allows for varied solar transmittance along the length of the river in response to riparian vegetation, and was modified for this recent modeling effort as described previously. The input for tree height was 22 feet at all nodes where vegetation was identified as present (Deas et al, 1997), which is the average tree height (Abbott, 2002). The longitudinal distribution of shade conditions on the Shasta River is presented in Figure 8 in Section 3.6.

Table 12. Calibrated P_{max} values assigned to NCRWQCB reaches

Reach (NCRWQCB Descriptor)	Benthic Cover %	River Mile		Relative Coverage	P_{max} gO ₂ /m ² /hour Calibrated
		From	To		
Riverside	35	39.27	40.47	med	2.36
Hidden Valley	75	32.06	39.27	high	3.15
E. Louie Road	70	30.57	32.06	high	3.15
u/s GID	85	25.85	30.57	high	3.15
d/s GID	40	24.11	25.85	med	2.36
15 - u/s A12	10	22.14	24.11	low	1.20
14 - A12 to DeSoza	15	16.08	22.14	med	2.36
De Soza to Brecada	70	14.74	16.08	high	3.15
Brecada to u/s Big Bend	10	13.8	14.74	low	1.20
Big Bend	90	13.31	13.8	high	3.15
d/s Big Bend to u/s Hwy3	30	12.63	13.31	med	2.36
u/s Hwy3 to impoundment	70	12.24	12.63	high	3.15
d/s impoundment - short reach	20	11.73	12.24	med	2.36
d/s impoundment to Y-A Rd	15	10.9	11.73	med	2.36
Y-A Rd to riparian	95	10.56	10.9	high	3.15
riparian to 263	50	6.36	10.56	med	2.36
263 to d/s Pioneer Bridge	5	4.23	6.36	low	1.20
d/s Pioneer Bridge to u/s USGS gage	25	4.05	4.23	med	2.36
USGS gage to mouth	5	0	4.05	low	1.20

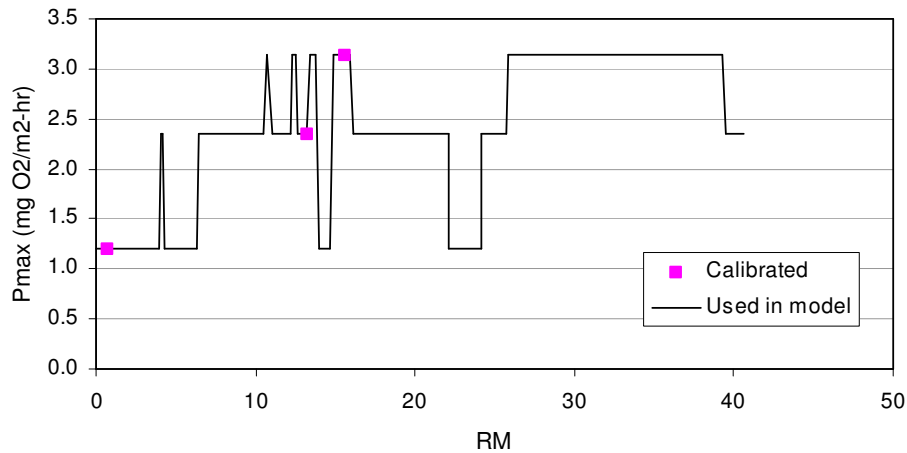


Figure 13. Calibrated values of P_{max} distributed by observed coverage along the Shasta River by river mile (RM)

Table 13. The spatial distribution of Pmax and respiration values for the July, August, and September simulation periods

River Mile	July 2-8		Aug 29-Sep 4		Sep 17-23	
	PMAX20	RESP20	PMAX20	RESP20	PMAX20	RESP20
40.62	2.36	0.48	2.36	0.48	2.36	0.24
39.51	2.36	0.48	2.36	0.48	2.36	0.24
39.26	3.15	0.64	3.15	0.64	3.15	0.32
25.85	3.15	0.64	3.15	0.64	3.15	0.32
25.79	2.36	0.48	2.36	0.48	2.36	0.24
24.11	2.36	0.48	2.36	0.48	2.36	0.24
24.10	1.20	0.24	1.20	0.24	1.20	0.12
22.14	1.20	0.24	1.20	0.24	1.20	0.12
22.13	2.36	0.48	2.36	0.48	2.36	0.24
16.11	2.36	0.48	2.36	0.48	2.36	0.24
15.91	3.15	0.64	3.15	0.64	3.15	0.32
14.88	3.15	0.64	3.15	0.64	3.15	0.32
14.68	1.20	0.24	1.20	0.24	1.20	0.12
13.99	1.20	0.24	1.20	0.24	1.20	0.12
13.79	3.15	0.64	3.15	0.64	3.15	0.32
13.40	3.15	0.64	3.15	0.64	3.15	0.32
13.26	2.36	0.48	2.36	0.48	2.36	0.24
12.63	2.36	0.48	2.36	0.48	2.36	0.24
12.58	3.15	0.64	3.15	0.64	3.15	0.32
12.27	3.15	0.64	3.15	0.64	3.15	0.32
12.16	2.36	0.48	2.36	0.48	2.36	0.24
11.10	2.36	0.48	2.36	0.48	2.36	0.24
10.69	3.15	0.64	3.15	0.64	3.15	0.32
10.55	2.36	0.48	2.36	0.48	2.36	0.24
6.42	2.36	0.48	2.36	0.48	2.36	0.24
6.34	1.20	0.24	1.20	0.24	1.20	0.12
4.30	1.20	0.24	1.20	0.24	1.20	0.12
4.19	2.36	0.48	2.36	0.48	2.36	0.24
4.05	2.36	0.48	2.36	0.48	2.36	0.24
3.98	1.20	0.24	1.20	0.24	1.20	0.12
0.00	1.20	0.24	1.20	0.24	1.20	0.12

6.0 Task 6: Calibration and Validation

Model calibration and validation for flow, temperature, and dissolved oxygen was completed for several discrete periods of time. The calibration period was 9/17/2002-9/23-2002 and the validations periods were 7/02/2002-7/08/2002 and 8/29/2002-9/04/2002. Model parameters were set during calibration and these values were retained during validation.

6.1 Flow

Representation of stream flows, as well as calibration procedures, are discussed in detail in the previous modeling memo (Deas and Geisler, 2004). The principal parameter

adjusted for flow calibration was Manning's roughness coefficient, n^2 . Figures Figure 14 through Figure 17, below, include simulated versus measured flow for several locations along the Shasta River for the calibration period. Daily trends are well represented; however, sub-daily deviations are apparent. These deviations are due to the daily water balance completed on a reach basis and do not account for intra-reach operations (diversions and return flows). Sub-daily deviations (e.g., hourly) are due to the averaging to daily values in completing the water balance exercise. Statistical summaries for each location are provided in Table 14 through Table 16. The root mean squared error (RMSE) for all locations is less than 3.0 cfs, with a mean absolute error (MAE) of less than 2.25 cfs.

Validation results for the 7/02/02-7/08/02 and 8/29/02-9/04/02 period are shown in Figure 18 through Figure 21 and Table 15, and Figure 22 through Figure 25 and Table 16, respectively. For the June period the RMSE and MAE is less than 4.5 cfs and 3.54 cfs, respectively. Late August and early September period flow statistics for RMSE and MAE were 2.78 cfs and 2.32 cfs, respectively.

In all cases model performance at the mouth showed the largest error statistics. Presumably the accumulation of uncertainty in return flows and diversions (both in space and time) in the downstream direction contribute to model performance. Overall these deviations are on the order of uncertainty associated with flow measurement in a system such as the Shasta River (USGS, 2005).

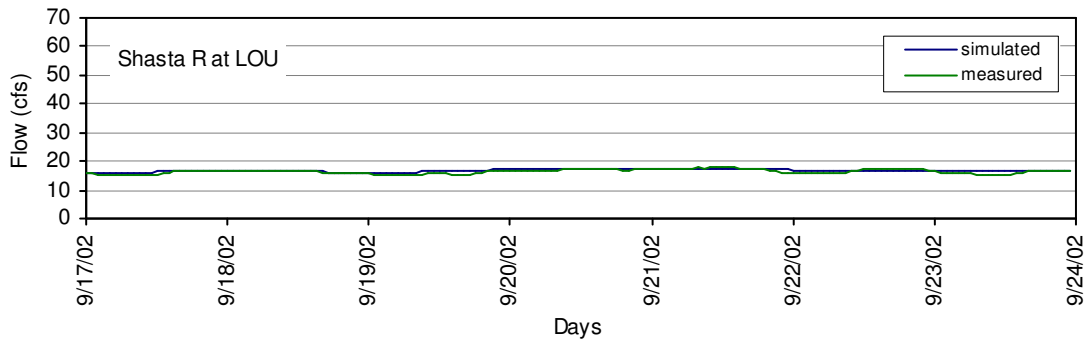


Figure 14. Flow at Louie Road from 9/17/02 – 9/23/02

² Shen and Julien (1993) present a wide range of Manning roughness coefficients various levels of particle size distributions (sand, gravels, cobbles), levels of vegetation, sinuosity, and channel gradient. Values generally range from 0.01 to 0.20 for various combinations of the above factors.

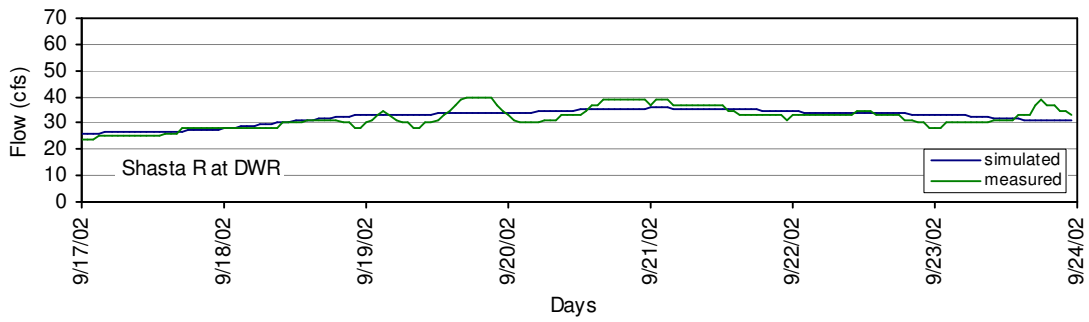


Figure 15. Flow at DWR Weir from 9/17/02 – 9/23/02

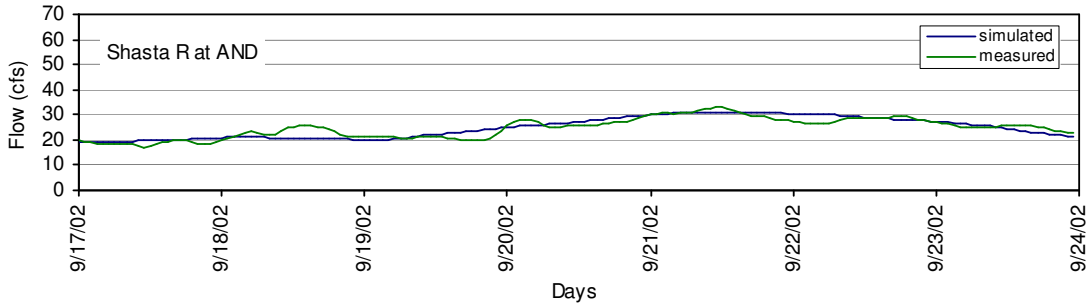


Figure 16. Flow at Anderson Grade from 9/17/02 – 9/23/02

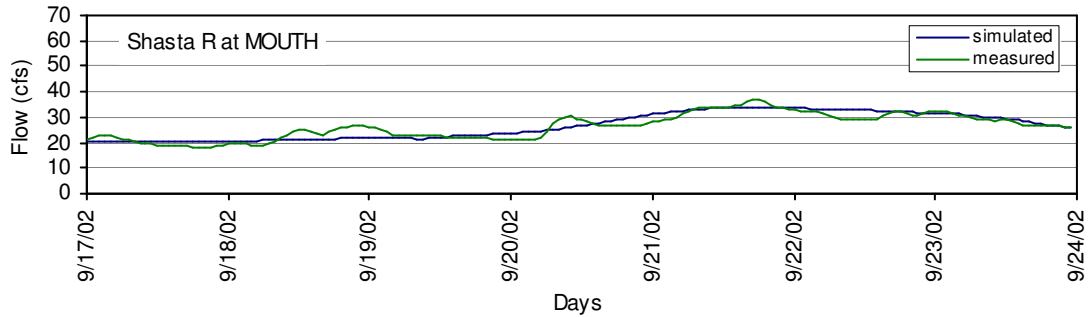


Figure 17. Flow at the Mouth from 9/17/02 – 9/23/02

Table 14. Statistics for final calibrated flow model for 9/17/02-9/23/02 with n = 0.05

Statistic (values in cfs)	Louie Rd. (RM 33.92)	DWR (RM 15.5)	Anderson Grade (RM 8.03)	Mouth (USGS gage) (RM 0.62)
Mean Bias	0.39	0.43	0.14	0.14
Mean absolute error (MAE)	0.51	2.22	1.53	1.70
Root mean squared error (RMSE)	0.63	2.75	1.92	2.12
number of hours in sample	168	168	168	168

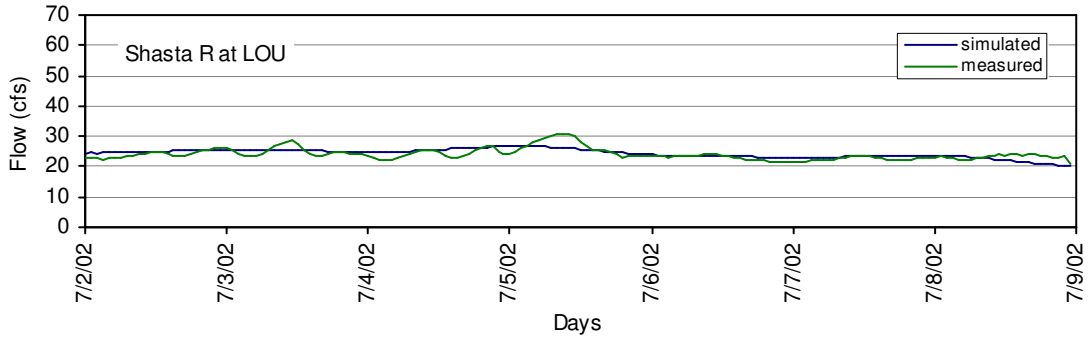


Figure 18. Flow at the Louie Road from 7/02/02 – 7/08/02

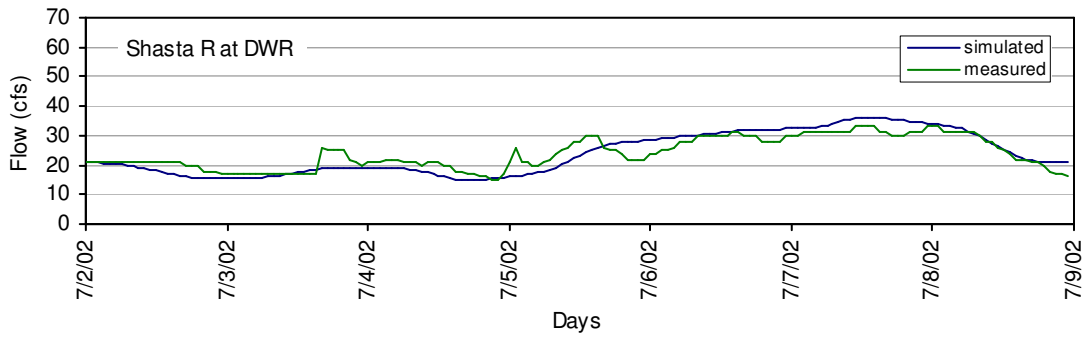


Figure 19. Flow at the DWR Weir from 7/02/02 – 7/08/02

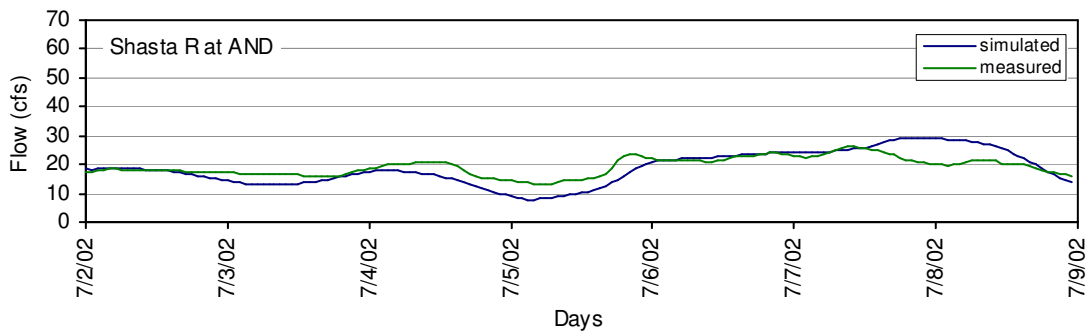


Figure 20. Flow at Anderson Grade from 7/02/02 – 7/08/02

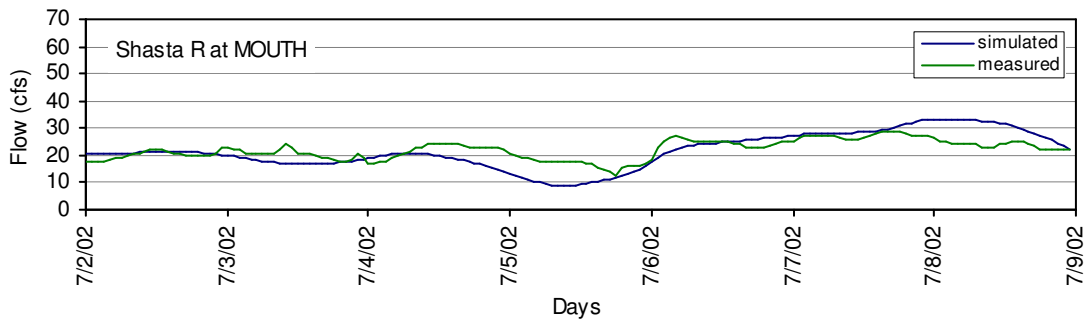


Figure 21. Flow at the Mouth from 7/02/02 – 7/08/02

Table 15. Statistics for flow model for validation period 7/02/02-7/08/02

Statistic (values in cfs)	Louie Rd. (RM 33.92)	DWR (RM 15.5)	Anderson Grade (RM 8.03)	Mouth (USGS gage) (RM 0.62)
Mean Bias	0.24	-0.15	-0.54	-0.40
Mean absolute error (MAE)	1.20	2.62	2.84	3.54
Root mean squared error (RMSE)	1.55	3.19	3.71	4.50
number of hours in sample	168	168	168	168

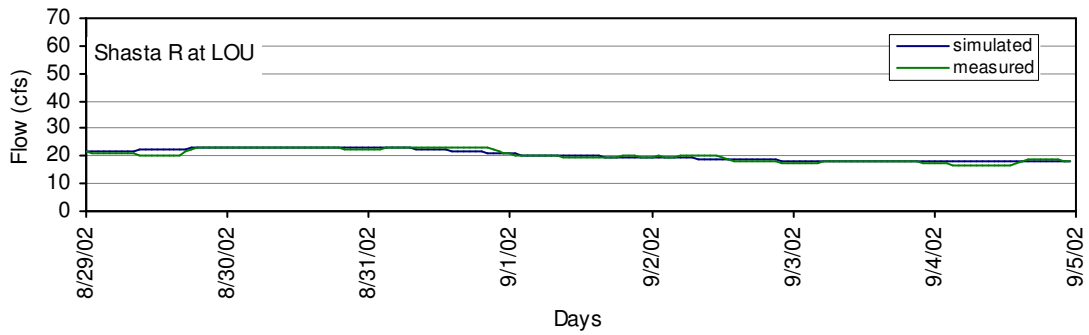


Figure 22. Flow at Louie Road from 8/29/02-9/04/02

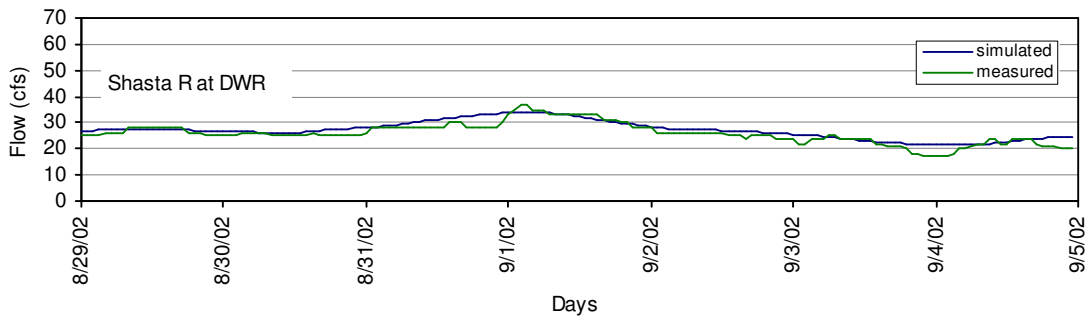


Figure 23. Flow at DWR Weir from 8/29/02-9/04/02

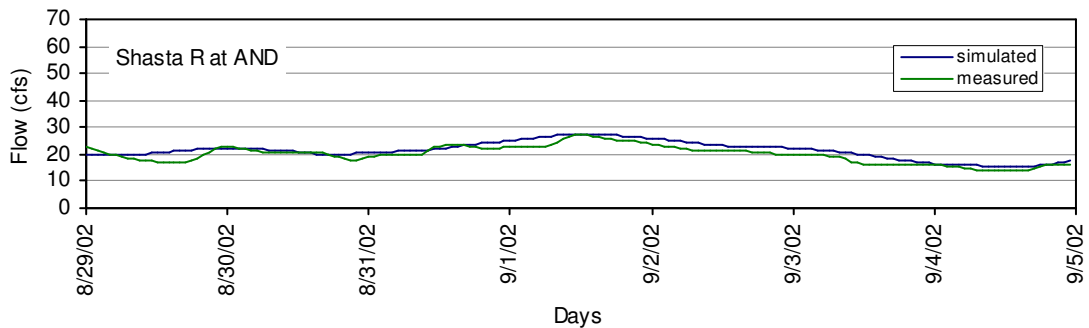


Figure 24. Flow at Anderson Grade from 8/29/02-9/04/02

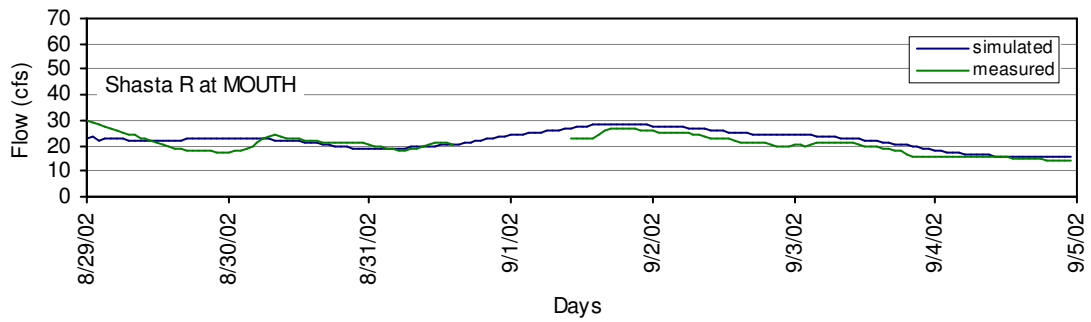


Figure 25. Flow at the Mouth from 8/29/02-9/04/02

Table 16. Statistics for flow model for validation period 8/29/02-9/04/02

Statistic (values in cfs)	Louie Rd. (RM 33.92)	DWR (RM 15.5)	Anderson Grade (RM 8.03)	Mouth (USGS gage) (RM 0.62)
Mean Bias	0.23	1.26	1.44	1.40
Mean absolute error (MAE)	0.63	1.66	1.67	2.32
Root mean squared error (RMSE)	0.81	2.11	1.95	2.79
number of hours in sample	168	168	168	168

6.2 Water Temperature

Water temperature calibration consisted primarily of modifying the evaporative heat flux coefficients, AA ($\text{m}^3/\text{mb}/\text{s}$) and BB (m^2/mb) for the equation $\psi = AA + BB \cdot \text{wind}$. The thermal diffusivity of bed material, K (cm^2/hr) was also modified, but ultimately set to the default value (Hauser, 2002).

Table 17. Final values for calibrated model

Coefficient	Value
AA	1E-9 $\text{m}^3/\text{mb}/\text{s}$
BB	1.5E-9 m^2/mb
n	0.05
K (DIF)	27.7 cm^2/hr

6.2.1 Instabilities in temperature

The original calibration based on previous geometry (Abbott, 2002) and different model parameters, resulted in modest instabilities (oscillations) in the temperature results during calibration (Figure 26). The RQUAL numerical solution in previous work was performed using a 4-point implicit scheme which can be subject to such instabilities. Increasing the spatial derivative weighting factor (theta) from 0.50 to 0.55 in was sufficient to dampen the oscillations in all simulations (Figure 27).

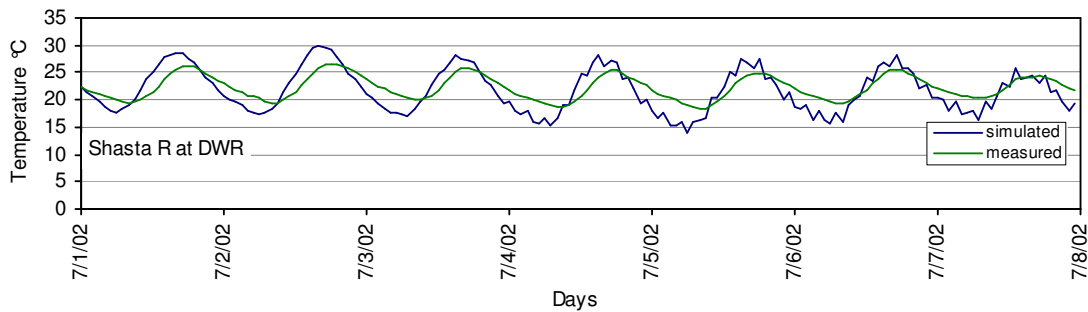


Figure 26. Temperature at DWR Weir for validation period 7/02/2002 – 7/08/2002 with theta = 0.5

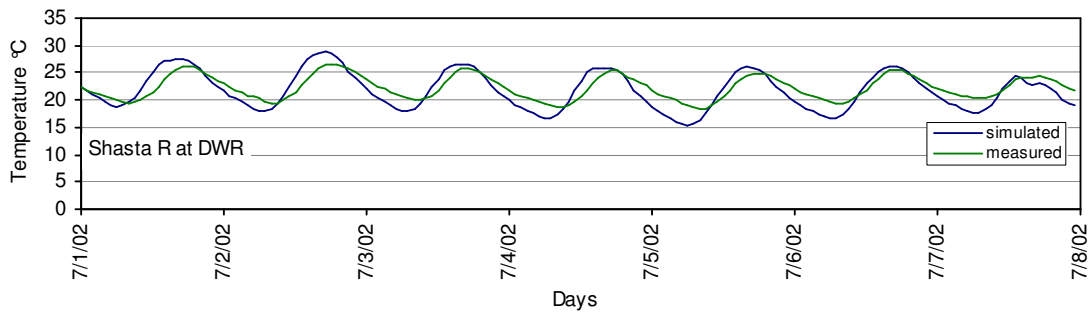


Figure 27. Temperature at DWR Weir for validation period 7/02/2002 – 7/08/2002 with theta = 0.55

These instabilities could not be resolved with theta values within the documented range of values (0.5-0.6) with the updated geometry (Lamphear) and increased number of nodes. Thus, the Holly-Priessman scheme was chosen as an alternate.

6.2.2 Results

Statistics for all calibration files for temperature calibration in Appendix 1.

Figure 28 through Figure 31 and Table 21 include simulated versus measured temperature for several locations along the Shasta River for the calibration period. Results for the validation periods are presented in Figure 32 through Figure 39 and Tables 22 and 23. Throughout the river model simulated T_w agrees well with measured data, including phase and amplitude. Model simulated temperature effectively captures the thermal dynamics of the Shasta River under a variety of summer and early-fall hydrologic and meteorological conditions in the Shasta River. Modeled temperatures in the upper reaches and valley reaches match the measured phase and amplitude of the daily temperature trace well – for all periods the RMSE and MAE for all sites above Yreka Creek are generally less than 2°C. Simulated values at the mouth are generally under-predicted, particularly for the daily minimum, and may lag in phase slightly. For the location near the mouth of the Shasta River RMSE range from 1.93°C to 3.59°C, and MAE range from 1.58°C to 3.3°C. One factor potentially influencing predicted temperatures at the mouth might be the fact that during summer and fall periods considerably different meteorological conditions occur in the canyon reach. Although the Shasta River canyon may provide a modest amount of topographic shading, the rocky canyon creates a hot, arid reach, with the canyon walls re-radiating heat well into the evening hours. Local meteorological data may improve model prediction capabilities in the lower portion of this reach if deemed necessary.

Another factor affecting water temperature conditions include water resources management actions in the valley reach by local landowners and irrigation districts. Diversions and return flows are largely unquantified, making short-term operations difficult to simulate. Of particular interest are the modes of return flow to the Shasta River, including direct surface inputs from canals or ditches, non-point surface and subsurface runoff from fields and irrigation activities adjacent to the river. These waters enter the river at various times and temperatures.

Finally, stream geometry plays a vital critical role in water temperature response. The Shasta River is a small stream, making it prone to rapid response to meteorological conditions. As the river falls to very low levels in the summer, it is difficult to predict its depth and width based on available information. A considerable effort has gone into constructing a geometry that is responsive to flow conditions, but in certain reaches data are limited.

Given the data limitations and challenges of addressing this small river system, overall model performance is good, providing critical insight into temperature dynamics along the river main stem from Dwinnell Reservoir to the confluence with the Klamath River.

These temperature results were used during model calibration for dissolved oxygen, and subsequently application of the model.

Table 18. Statistics for final calibrated temperature model for period 9/17/02-9/23/02

Statistic (values in °C)	Louie Rd. (RM 33.92)	DWR (RM 15.5)	Anderson Grade (RM 8.03)	Mouth (USGS gage) (RM 0.62)
Mean Bias	0.09	0.02	-0.47	-0.71
Mean absolute error (MAE)	0.59	0.69	1.29	1.58
Root mean squared error (RMSE)	0.73	0.90	1.56	1.93
number of hours in sample	168	168	168	168

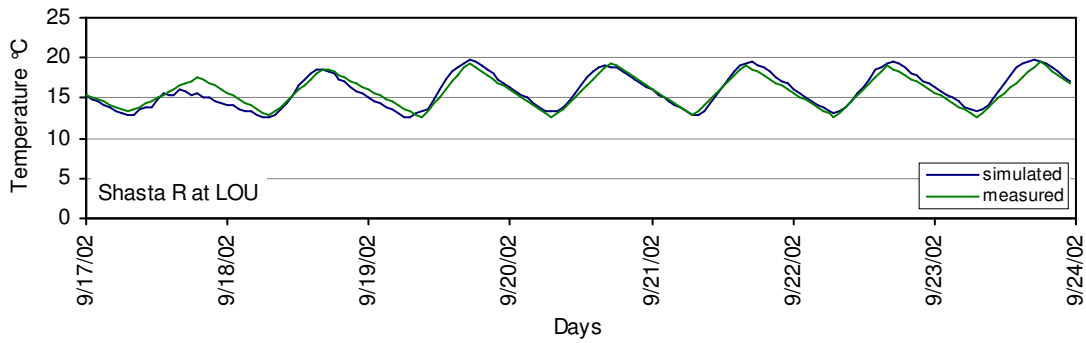


Figure 28. Temperature at Louie Road for 9/17/02 – 9/23/02

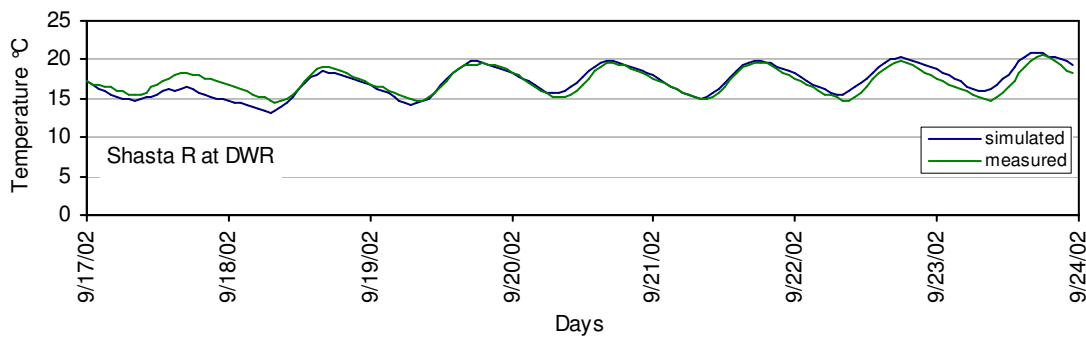


Figure 29. Temperature at DWR Weir for 9/17/02 – 9/23/02

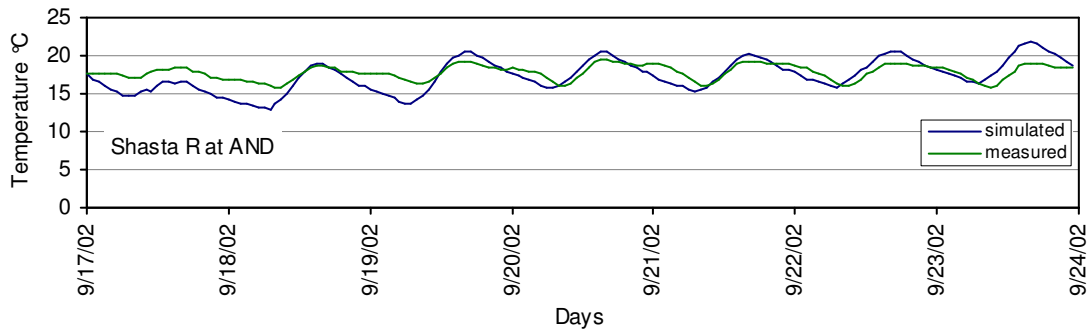


Figure 30. Temperature at Anderson Grade for 9/17/02 – 9/23/02

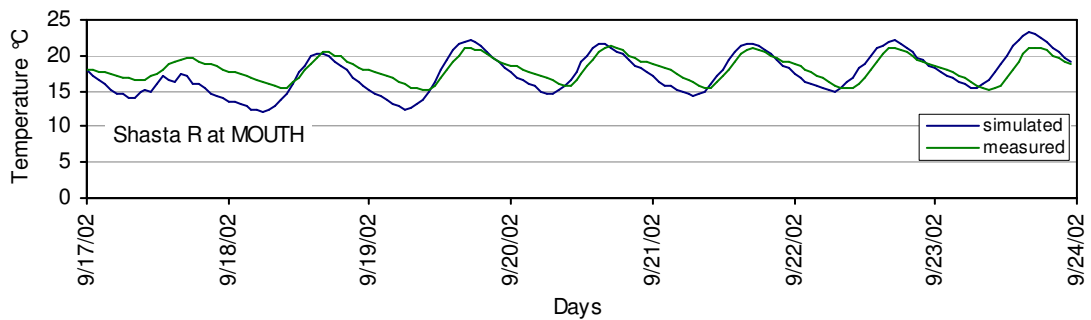


Figure 31. Temperature at the Mouth for 9/17/02 – 9/23/02

Table 19. Statistics for temperature model for validation period 7/02/02-7/08/02

Statistic (values in °C)	Louie Rd. (RM 33.92)	DWR (RM 15.5)	Anderson Grade (RM 8.03)	Mouth (USGS gage) (RM 0.62)
Mean Bias	0.84	-0.62	-1.33	-1.40
Mean absolute error (MAE)	1.15	1.09	1.57	1.94
Root mean squared error (RMSE)	1.41	1.36	2.02	2.38
number of hours in sample	168	168	168	168

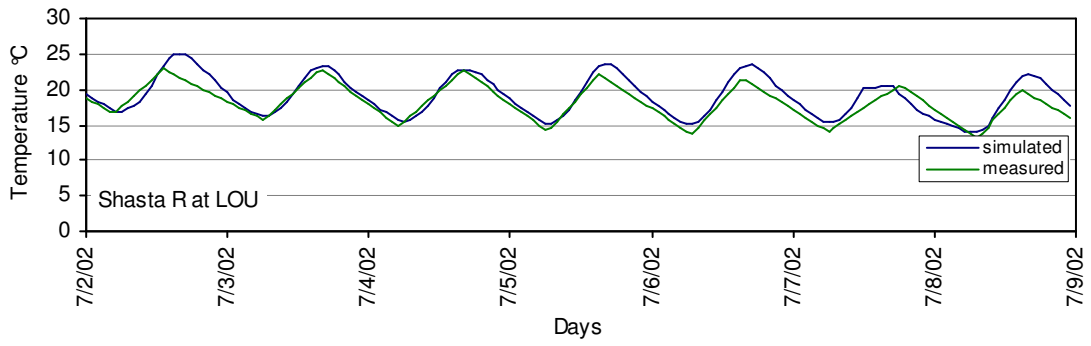


Figure 32. Temperature at Louie Road for period 7/02/02 – 7/08/02

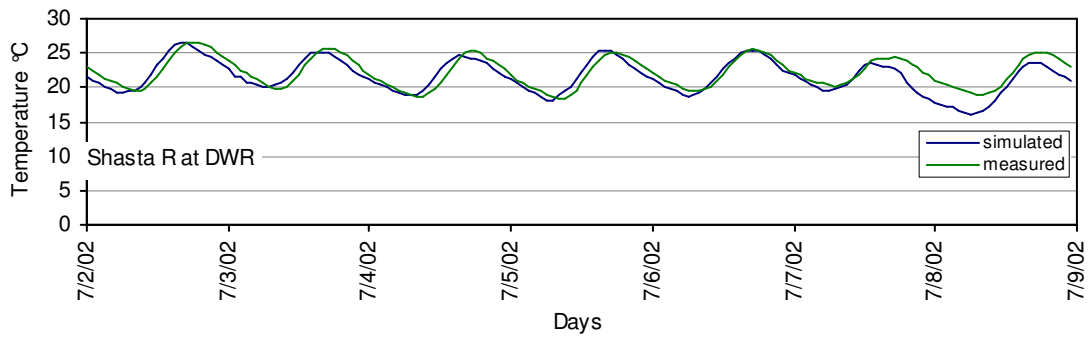


Figure 33. Temperature at DWR Weir for period 7/02/02 – 7/08/02

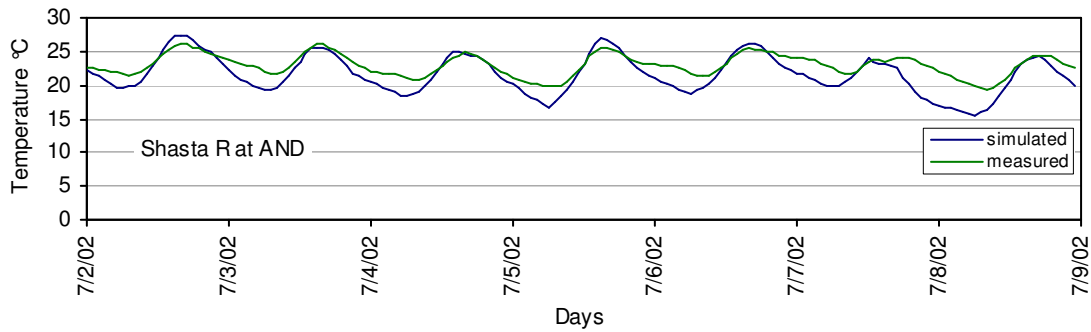


Figure 34. Temperature at Anderson Grade for period 7/02/02 – 7/08/02

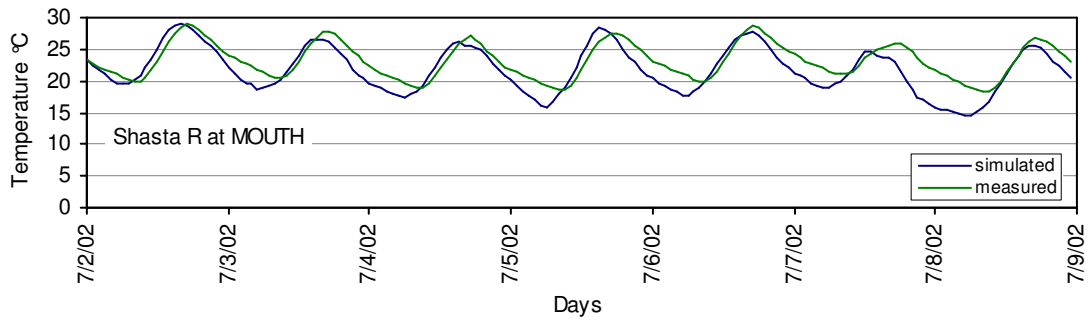


Figure 35. Temperature at the Mouth for period 7/02/02 – 7/08/02

Table 20. Statistics for temperature model for validation period 8/29/02-9/04/02

Statistic (values in °C)	Louie Rd. (RM 33.92)	DWR (RM 15.5)	Anderson Grade (RM 8.03)	Mouth (USGS gage) (RM 0.62)
Mean Bias	0.27	-0.34	-1.29	-3.30
Mean absolute error (MAE)	1.76	0.97	1.64	3.30
Root mean squared error (RMSE)	2.16	1.34	2.10	3.59
number of hours in sample	168	168	168	168

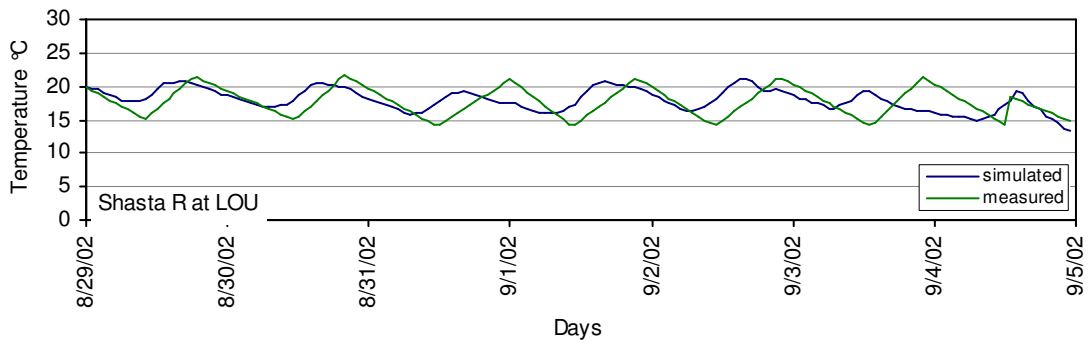


Figure 36. Temperature at Louie Road for period 8/29/02-9/04/02

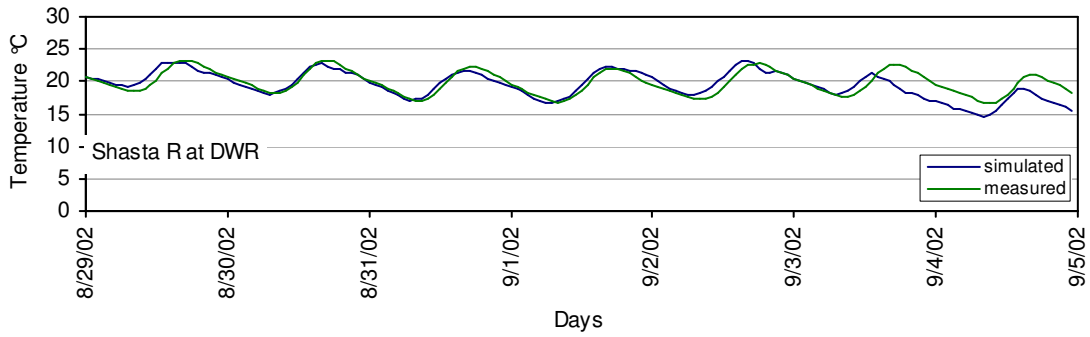


Figure 37. Temperature at DWR Weir for period 8/29/02-9/04/02

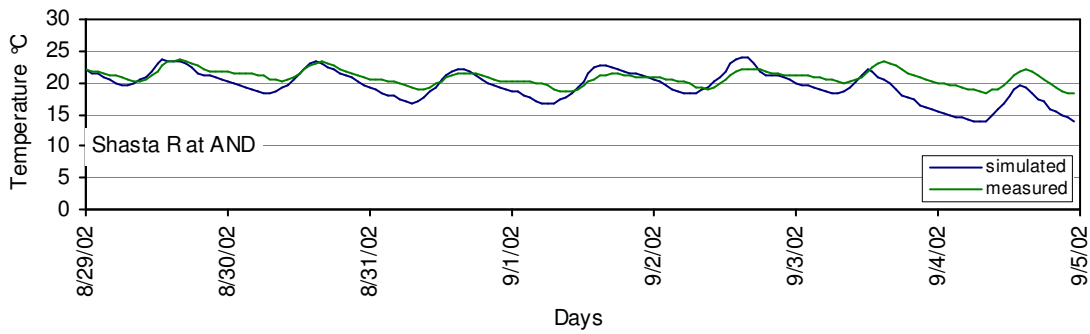


Figure 38. Temperature at Anderson Grade for period 8/29/02-9/04/02

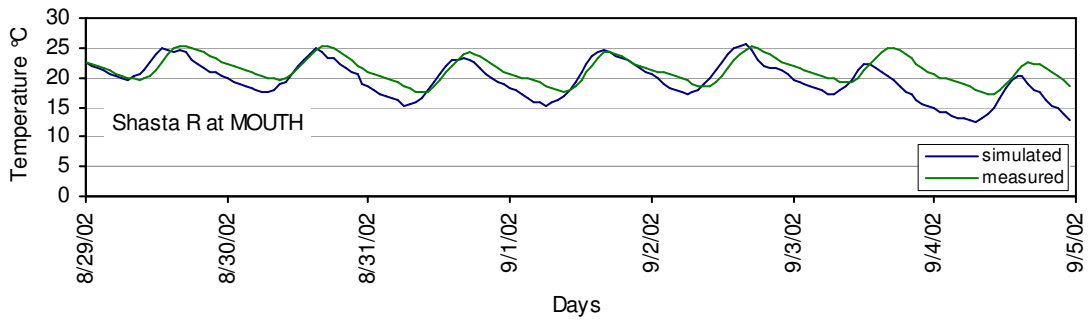


Figure 39. Temperature at the Mouth for period 8/29/02-9/04/02

6.3 Dissolved Oxygen

Water quality calibration consisted of modifying parameters to reproduce dissolved oxygen. The RQUAL model simulates dissolved oxygen conditions in response to biochemical oxygen demand (BOD), nitrogenous biochemical oxygen demand (NBOD), sediment oxygen demand (SOD), mechanical reaeration, and photosynthesis and respiration of algae growing on or in the bed (as macrophytes or periphyton). Specification of CBOD, NBOD, SOD, reaeration, photosynthesis and respiration, and riparian shading for the Shasta River were presented in previous sections of the report.

Model coefficients, rates, and parameters that are associated with these processes can have a direct influence on simulated dissolved oxygen conditions. For example CBOD, NBOD, and SOD decay rates can influence the rate of oxygen demand placed on the system. Likewise, reaeration formulations (rate) can influence the amount of reoxygenation or deoxygenation across the air water interface due to mechanical reaeration. Finally, photosynthesis and respiration by aquatic plants have direct implications on oxygen concentrations in the water column during daytime and nighttime periods. Dissolved oxygen for the Shasta River was calibrated using data for the periods 9/17/02 – 9/23/02 at Montague-Grenada Road, Highway 3, and the mouth. Data were unavailable from upstream locations. Although a wide range of parameters were explored during calibration (see available parameters in Table 8), the model was most responsive to photosynthetic and respiration rates. The calculated rates listed in Table 21 were applied in the calibration process.

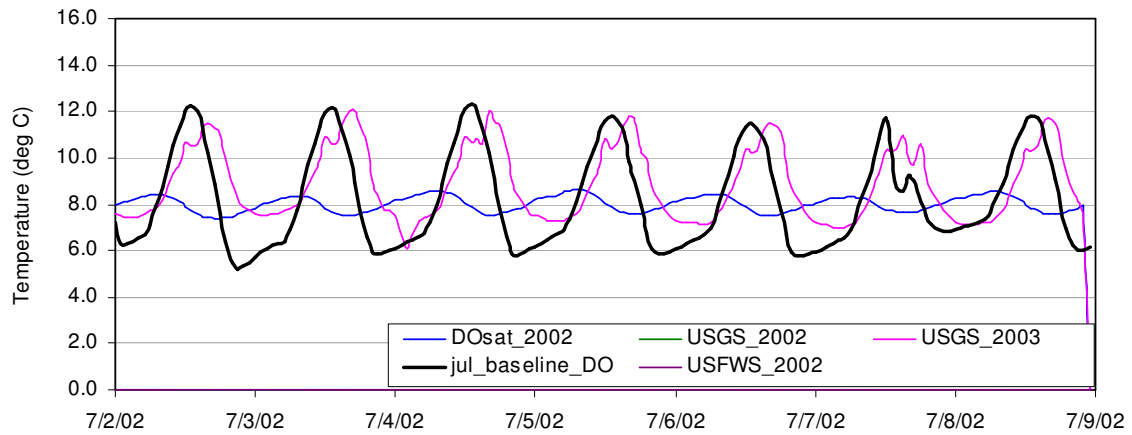
One of the primary challenges during dissolved oxygen calibration was working with limited data sets and there is uncertainty associated with data sets (see USGS, 2005). As a result, 2003 data was used to augment available data and assist in assessing model performance. The basic assumption is that flow, meteorological, and aquatic/benthic conditions were roughly similar between the two years.

Calibrated model parameters provided in Table 8 and for macrophyte maximum photosynthetic rate and respiration are shown in Table 24. The results are presented for Montague Grenada Road (DWR Weir), Highway 3, and the mouth in Figure 40 through **Error! Reference source not found.**, representing July, late August, and September time periods, respectively.

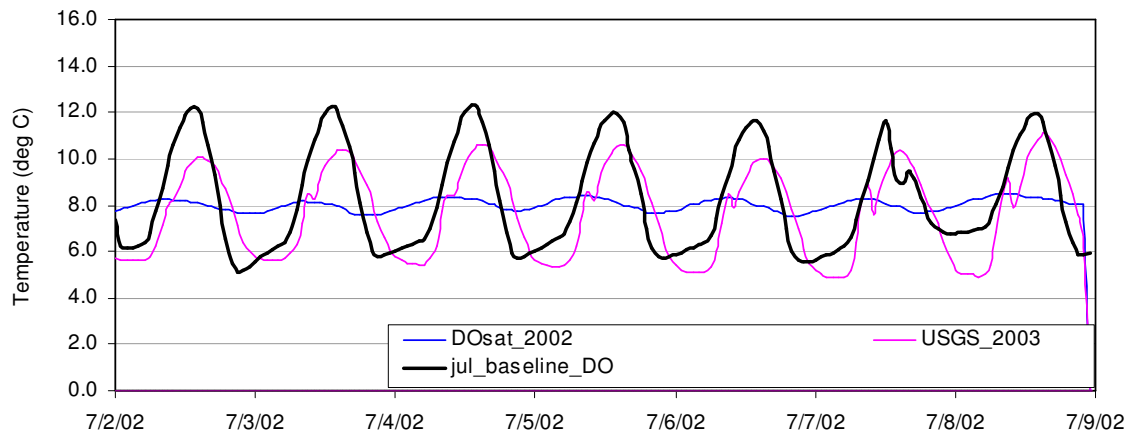
Overall, the model performance is quite good, replicating the phase and amplitude of dissolved oxygen conditions in the river. For July, daily maximum values at Highway 3 are overestimated by approximately 1.5 mg/l, while minimum daily values are well represented. There is a slight phase shift at Highway 3 and DWR Weir in July as well. Late August and September are well represented. For all of the periods, field data at the mouth confound comparison with simulated values. 2003 data is included as an additional source of insight. In theory, the canyon should provide mechanical reaeration through the steep riverine reach. Simulated results agree well with saturation dissolved oxygen values and 2003 USGS data. The USFWS and USGS data, although within agreement of less than 1.0 mg/l in late July, deviate remarkably in September. Given that there were identified data issues with the USGS data in 2002 (USGS, 2005), efforts were not taken to match these data sets. Due to the limited calibration data from the year in questions, calibration statistics are not included for dissolved oxygen.

Table 21. Calibrated model parameters for photosynthetic rate (Pmax) and respiration rate

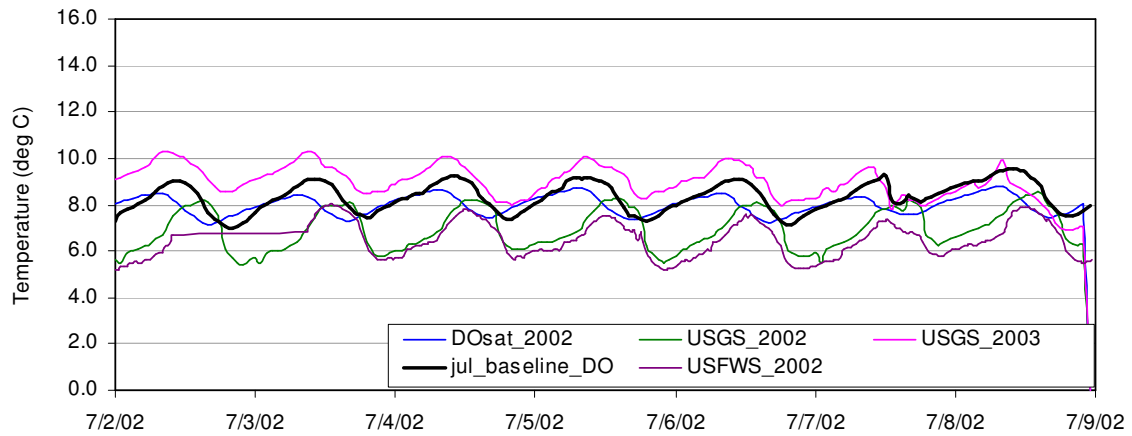
River Mile	Respiration (gO2/m2/hour)	Pmax (gO2/m2/hour)
40.62	0.24	2.36
39.26	0.24	2.36
39.19	0.31	3.15
25.86	0.31	3.15
25.79	0.24	2.36
24.11	0.24	2.36
24.10	0.24	2.36
22.14	0.24	2.36
22.13	0.24	2.36
16.11	0.24	2.36
15.91	0.31	3.15
14.88	0.31	3.15
14.68	0.24	2.36
13.79	0.24	2.36
13.74	0.31	3.15
13.40	0.31	3.15
13.26	0.24	2.36
12.63	0.24	2.36
12.58	0.31	3.15
12.27	0.31	3.15
12.16	0.24	2.36
11.10	0.24	2.36
10.69	0.31	3.15
10.55	0.31	3.15
10.49	0.24	2.36
6.34	0.24	2.36
6.17	0.24	2.36
4.30	0.24	2.36
4.19	0.24	2.36
4.05	0.24	2.36
3.98	0.24	2.36
0.0	0.24	2.36



(a)

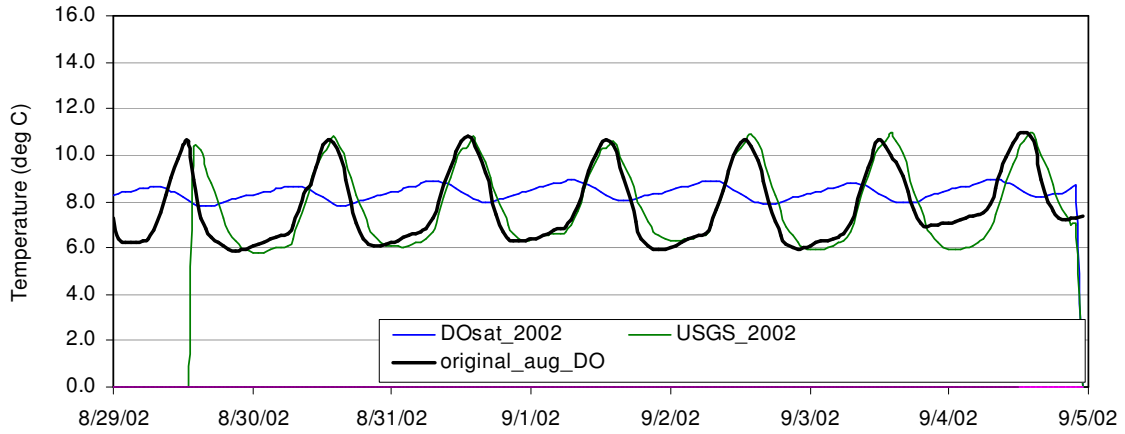


(b)

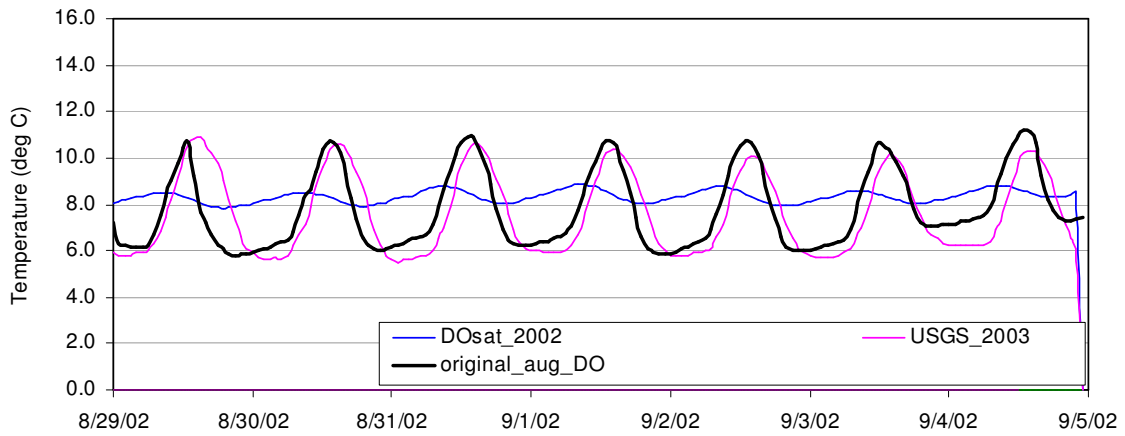


(c)

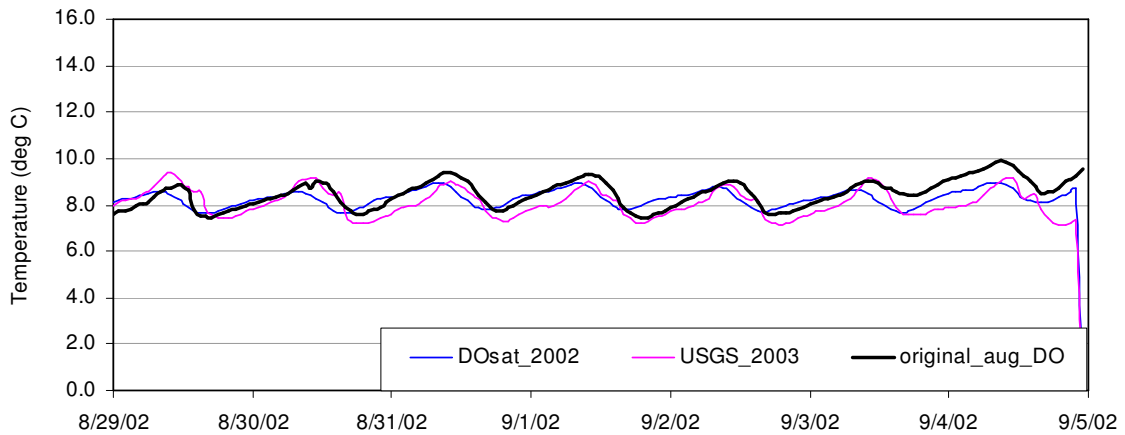
Figure 40. Simulated versus measured dissolved oxygen at (a) DWR Weir, (b) Highway 3, and (c) Mouth: 7/02/02-7/08/02



(a)

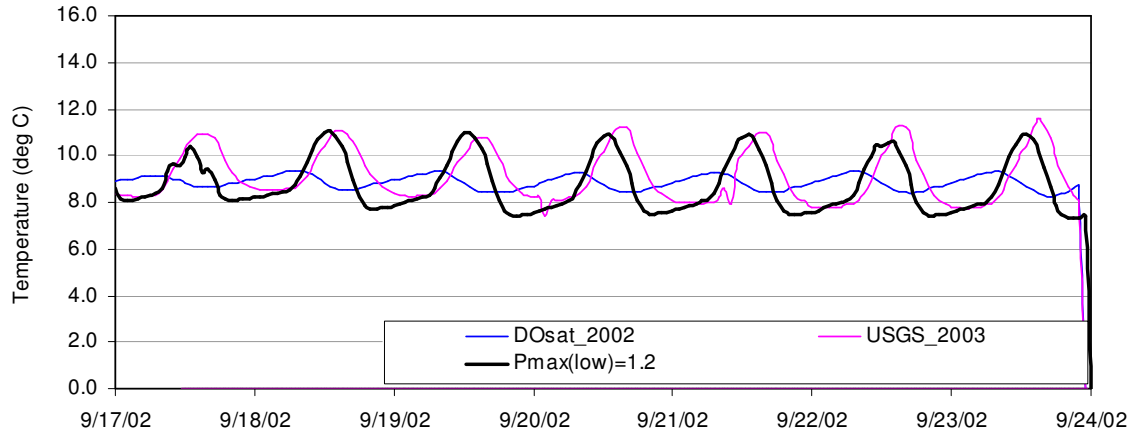


(b)

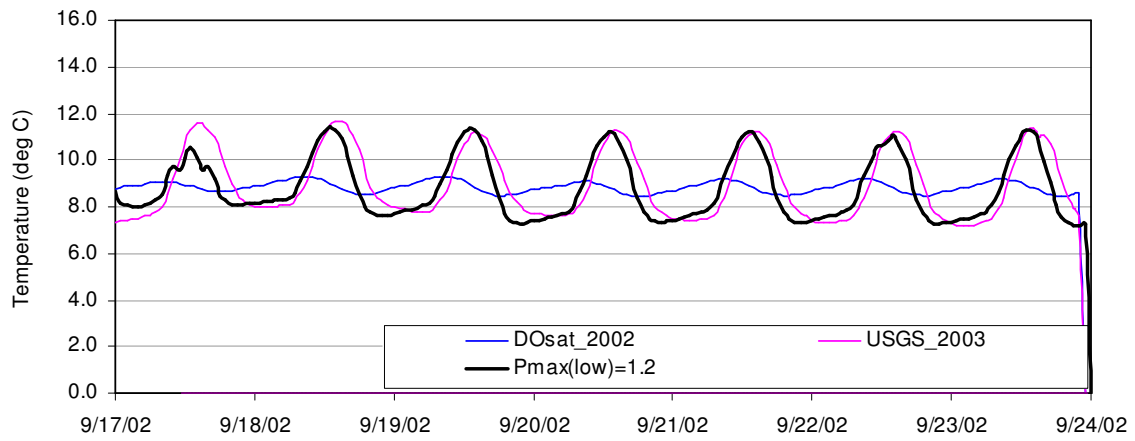


(c)

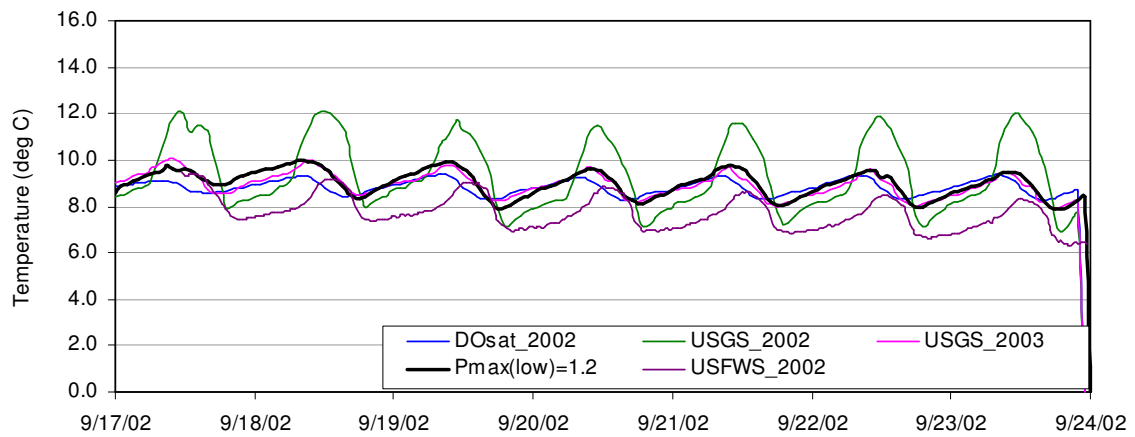
Figure 41. Simulated versus measured dissolved oxygen at (a) DWR Weir, (b) Highway 3, and (c) Mouth: 8/29/02-9/5/02



(a)



(b)



(c)

Figure 42. Simulated versus measured dissolved oxygen at (a) DWR Weir, (b) Highway 3, and (c) Mouth: 9/17/02-9/24/05

7.0 Sensitivity Analysis

Previous applications of the TVA RMS to the Shasta River included sensitivity analysis. Watercourse Engineering (2004b) and Abbott (2002) examined the impact of variable flow regimes and temperature boundary conditions on the transit time, depth, and thermal response of the river. An extensive effort was completed on examining the effects of various transmittance rates and tree heights, as well as the implications of variable flow regimes and spatial extent of riparian vegetation shading. The reader is referred to Watercourse Engineering (2004b) and Abbott (2002) for additional details.

Additional sensitivity analyses were completed under this project to identify the sensitivity of flow to Manning roughness, evaporative heat flux values, CBOD decay rate, NBOD decay rate, and selected SOD values. In sum, the model was modestly sensitive to manning roughness, primarily because the travel time through the system is relatively short (e.g., on the order of one day). As is typical in water temperature simulations, the model was sensitive to the evaporative heat flux coefficients used in the heat budget formulation. With respect to dissolved oxygen, CBOD, and NBOD decay rates were largely insensitive, as was the SOD rate. The driving factor for dissolved oxygen was maximum photosynthetic and respiration rate. These values were adjusted during calibration to fit the model to measured data. Reaeration rate, a calculated term within the model, played a pivotal role, particularly in the steep canyon reach where mechanical reaeration would be expected to occur. The results of these analyses are included in the Appendix. The results of these analyses assisted in calibration of the model and should assist decision makers in model interpretation.

8.0 References

- Abbott, A. G. P. 2002. *The Effect of Riparian Vegetation on Stream Temperature in the Shasta River*. Master's Paper. University of California, Davis. Department of Civil and Environmental Engineering.
- Anderson, Jeff and Don Huggins. 2003. *Production Calculator, version 1.5 Operations Manual*. Central Plains Central for BioAssessment, Kansas Biological Survey, University of Kansas. flipper@ku.edu or dhuggins@ku.edu
- California Department of Fish and Game (CDFG) Northern California-North coast Region (Region 1). *A Biological Needs Assessment for Anadromous Fish in the Shasta River Siskiyou County, California*. July, 1997.
- California Regional Water Quality Control Board North Coast Region (CRWQCB). 2005. *Shasta River Water Quality Investigations - 2004*. April.
- California Regional Water Quality Control Board North Coast Region (CRWQCB). 2004a. *Shasta River Water Quality Conditions 2002 & 2003*. May.
- California Regional Water Quality Control Board (CRWQCB). 2004b. *Shasta River TMDL Technical Memo #2 – Selection of Lamphear Hydrography for Water Quality Model*. November 1.
- California Regional Water Quality Control Board (CRWQCB). 2004c. *Shasta River Dissolved Oxygen TMDL Technical Memo #1: Sediment Oxygen Demand Rates*. October 26.
- Chapra, Steven C. 1997. *Surface Water-Quality Modeling*. McGraw-Hill, New York.
- Deas, M.L. and L. Geisler. 2005. “Completion of the Shasta River Flow and Temperature Modeling Phase.” Technical Memorandum. to Joshua Viers, John Muir Institute of the Environment, University of California, Davis. September 13.
- Deas, M.L. and G.T. Orlob. 1997. *Shasta River Data Inventory*. Clean Water Act 205(j) Grant Program, California State Water Resources Control Board and the Shasta Valley Resources Conservation District. June.
- Deas, M.L., J. Haas, and G.T. Orlob. 1997. *Shasta River Woody Riparian Vegetation Inventory*. Clean Water Act 205(j) Grant Program, California State Water Resources Control Board and the Shasta Valley Resources Conservation District. June.
- Hauser, G.E. and G.A. Schohl. 2002. *River Modeling System v4 – User Guide and Technical Reference*. Report No. WR28-1-590-164. TVA River System Operations and Environment. Norris, Tennessee. May.

- Lowney, C.L. 2000. *River Temperature Dynamics in the Sacramento River: Measuring and Monitoring*. Ph.D. Dissertation, Department of Civil and Environmental Engineering, University of California, Davis.
- Monteith, J.L. and M. Unsworth. 1990. *Principles of Environmental Physics*, 2nd Edition. London, England: Edward Arnold.
- Shen, H.W. and P.Y. Julien. “Chapter 12: Erosion and Sediment Transport” in *Handbook of Hydrology*. Ed. D. R. Maidment. McGraw Hill, Inc. New York.
- Thomann, R.V. and J.A. Mueller. 1987. *Principles of Surface Water Quality Modeling and Control*. Harper & Row, New York.
- United States Geological Survey. 2005. *Water Quality Data from 2002 to 2003 and analysis of Data Gaps for Development of Total Maximum Daily Loads in the Lower Klamath River Basin, California*. Prepared by L. E. Flint, A.L. Flint, D.S. Curry, S.A. Rounds, and M.C. Doyle. Scientific Investigations Report 2004-5255.
- Watercourse Engineering, Inc. 2004a. *Shasta River Field Monitoring Report*. Deas, M.L. and A.G. Abbott. Prepared for the Klamath River Basin Fisheries Task Force and the United States Fish and Wildlife Service. November.
- Watercourse Engineering, Inc. 2004b. *Shasta River Flow and Temperature Modeling Report*. Prepared for the California Department of Fish and Game. November.
- Watercourse Engineering. 2002. *Pond Equilibrium Temperature Model: Assumptions and User’s Guide*. Internal Memo 8/30/2002.
- Watercourse Engineering. 2002b. *Incremental Shading Analysis, Shasta River*. May 1. Prepared for the Shasta Valley Resource Conservation District.

Personal Communications

Merlynn Bender, U.S. Bureau of Reclamation, Denver Technical Services Center
Cindy Lowney, Consultant

9.0 Appendix: Sensitivity Analysis Results

9.1 Manning Roughness

Flow simulation was tested for sensitivity with respect to the Manning roughness coefficient. The coefficient was varied from 0.04 to 0.055 in increments of 0.005. Statistical summaries of model performance under the various roughness values are shown in Table 22 through Figure 25. Results indicate that the model performed similarly in all cases. The relatively short transit time through the model domain, coupled with the representation of accretions and depletions on a reach basis (based on

the daily water balance) results in the model being generally insensitive to the Manning roughness coefficient.

Table 22. Statistics for final calibrated flow model for 9/17/02-9/23/02 with n = 0.05

	Louie Rd. (RM 33.92)	DWR (RM 15.5)	Anderson Grade (RM 8.03)	Mouth (USGS gage) (RM 0.62)
Mean Bias	0.39	0.43	0.14	0.14
Mean absolute error (MAE)	0.51	2.22	1.53	1.70
Root mean squared error (RMSE)	0.63	2.75	1.92	2.12
number of hours in sample	168	168	168	168

Table 23. Statistics for flow model for 9/17/02-9/23/02 with n = 0.055

	Louie Rd. (RM 33.92)	DWR (RM 15.5)	Anderson Grade (RM 8.03)	Mouth (USGS gage) (RM 0.62)
Mean Bias	0.38	0.41	0.13	0.12
Mean absolute error (MAE)	0.51	2.22	1.52	1.71
Root mean squared error (RMSE)	0.63	2.75	1.91	2.14
number of hours in sample	168	168	168	168

Table 24. Statistics for flow model for 9/17/02-9/23/02 with n = 0.045

	Louie Rd. (RM 33.92)	DWR (RM 15.5)	Anderson Grade (RM 8.03)	Mouth (USGS gage) (RM 0.62)
Mean Bias	0.39	0.44	0.16	0.17
Mean absolute error (MAE)	0.51	2.22	1.53	1.70
Root mean squared error (RMSE)	0.64	2.74	1.91	2.11
number of hours in sample	168	168	168	168

Table 25. Statistics for flow model for 9/17/02-9/23/02 with n = 0.04

	Louie Rd. (RM 33.92)	DWR (RM 15.5)	Anderson Grade (RM 8.03)	Mouth (USGS gage) (RM 0.62)
Mean Bias	0.39	0.43	0.14	0.14
Mean absolute error (MAE)	0.51	2.22	1.53	1.70
Root mean squared error (RMSE)	0.63	2.75	1.92	2.12
number of hours in sample	168	168	168	168

9.2 Evaporative Heat Flux Coefficients and Bed Conduction

Evaporative heat flux parameters aa and bb (coefficients in the wind speed function for evaporative cooling ($\psi = aa + bb \cdot \text{wind}$)) were varied for various values and combinations. Recall, the selected values for aa and bb were $1.0 \times 10^{-9} \text{ m}^3/\text{mb/s}$ and $1.5 \times 10^{-9} \text{ m}^2/\text{mb}$, respectively. The results, presented in Appendix A, indicate that the model is sensitive to evaporative heat flux coefficients in the range of applicable values.

Sensitivity of temperature to calibrated aa and bb values for various bed thermal diffusivity values (DIF, represented by K). The calibrated value of K was $27 \text{ cm}^2/\text{hr}$ and values of $25 \text{ cm}^2/\text{hr}$ and $30 \text{ cm}^2/\text{hr}$ were assessed. Results showed modest sensitivity.

Finally, sensitivity of temperature to calibrated aa, bb, and K values for Manning roughness values of 0.045 to 0.055 were examined. Results, tabulated in Table 26, generally showed modest sensitivity.

Table 26. Summary of tables presenting sensitivity results

Table	aa ($\times 10^{-9} \text{ m}^3/\text{mb/s}$)	bb ($\times 10^{-9} \text{ m}^2/\text{mb}$)	K (cm^2/hr)	n
Table 27	0.5	1.5	27.7	0.05
Table 28	0.0	1.0	27.7	0.05
Table 29	1.0	1.5	27.7	0.05
Table 30	1.0	1.0	27.7	0.05
Table 31	0.5	1.0	27.7	0.05
Table 32	1.0	2.0	27.7	0.05
Table 33	2.0	2.0	27.7	0.05
Table 34	0.5	1.5	30.0	0.05
Table 35	0.5	1.5	25.0	0.05
Table 36	0.5	1.5	27.7	0.055
Table 37	0.5	1.5	27.7	0.045

Table 27. aa=0.5 bb= 1.5 (suggested values from User Guide)

	Louie Rd. (RM 33.92)	DWR (RM 15.5)	Anderson Grade (RM 8.03)	Mouth (USGS gage) (RM 0.62)
Mean Bias	0.33	0.32	-0.11	-0.30
Mean absolute error (MAE)	0.69	1.00	1.46	1.72
Root mean squared error (RMSE)	0.83	1.17	1.75	2.08
number of hours in sample	168	168	168	168

Table 28. aa=0.0 bb= 1.0

	Louie Rd. (RM 33.92)	DWR (RM 15.5)	Anderson Grade (RM 8.03)	Mouth (USGS gage) (RM 0.62)
Mean Bias	0.90	2.61	1.29	1.42
Mean absolute error (MAE)	1.04	1.71	2.13	2.48
Root mean squared error (RMSE)	1.20	1.87	2.42	2.85
number of hours in sample	168	168	168	168

Table 29. aa=1.0 bb= 1.5

	Louie Rd. (RM 33.92)	DWR (RM 15.5)	Anderson Grade (RM 8.03)	Mouth (USGS gage) (RM 0.62)
Mean Bias	0.10	-0.09	-0.64	-0.93
Mean absolute error (MAE)	0.59	0.77	1.41	1.72
Root mean squared error (RMSE)	0.73	0.99	1.73	2.11
number of hours in sample	168	168	168	168

Table 30. aa=1.0 bb= 1.0

	Louie Rd. (RM 33.92)	DWR (RM 15.5)	Anderson Grade (RM 8.03)	Mouth (USGS gage) (RM 0.62)
Mean Bias	0.38	0.38	-0.01	-0.16
Mean absolute error (MAE)	0.68	0.96	1.42	1.69
Root mean squared error (RMSE)	0.81	1.09	1.68	2.01
number of hours in sample	168	168	168	168

Table 31. aa=0.5 bb= 1.0

	Louie Rd. (RM 33.92)	DWR (RM 15.5)	Anderson Grade (RM 8.03)	Mouth (USGS gage) (RM 0.62)
Mean Bias	0.63	0.83	0.60	0.57
Mean absolute error (MAE)	0.84	1.30	1.67	1.93
Root mean squared error (RMSE)	0.98	1.43	1.94	2.27
number of hours in sample	168	168	168	168

Table 32. aa=1.0 bb= 2.0

	Louie Rd. (RM 33.92)	DWR (RM 15.5)	Anderson Grade (RM 8.03)	Mouth (USGS gage) (RM 0.62)
Mean Bias	-0.15	-0.50	-1.19	-1.56
Mean absolute error (MAE)	0.58	0.82	1.58	1.93
Root mean squared error (RMSE)	0.76	1.09	1.95	2.40
number of hours in sample	168	168	168	168

Table 33. aa=2.0 bb= 2.0

	Louie Rd. (RM 33.92)	DWR (RM 15.5)	Anderson Grade (RM 8.03)	Mouth (USGS gage) (RM 0.62)
Mean Bias	-0.54	-1.16	-2.00	-2.45
Mean absolute error (MAE)	0.68	1.19	2.08	2.53
Root mean squared error (RMSE)	0.89	1.40	2.45	2.97
number of hours in sample	168	168	168	168

Table 34. aa=1.0 bb= 1.5 K=30.0

	Louie Rd. (RM 33.92)	DWR (RM 15.5)	Anderson Grade (RM 8.03)	Mouth (USGS gage) (RM 0.62)
Mean Bias	0.11	-0.08	-0.64	-0.92
Mean absolute error (MAE)	0.59	0.76	1.42	1.73
Root mean squared error (RMSE)	0.73	0.98	1.73	2.11
number of hours in sample	168	168	168	168

Table 35. aa=1.0 bb= 1.5 K=25.0

	Louie Rd. (RM 33.92)	DWR (RM 15.5)	Anderson Grade (RM 8.03)	Mouth (USGS gage) (RM 0.62)
Mean Bias	0.09	-0.10	-0.66	-0.94
Mean absolute error (MAE)	0.59	0.78	1.41	1.71
Root mean squared error (RMSE)	0.73	1.01	1.74	2.11
number of hours in sample	168	168	168	168

Table 36. aa=1.0 bb= 1.5 K=27.7 n = 0.055

	Louie Rd. (RM 33.92)	DWR (RM 15.5)	Anderson Grade (RM 8.03)	Mouth (USGS gage) (RM 0.62)
Mean Bias	0.11	-0.08	-0.63	-0.91
Mean absolute error (MAE)	0.59	0.77	1.44	1.68
Root mean squared error (RMSE)	0.72	0.99	1.75	2.07
number of hours in sample	168	168	168	168

Table 37. aa=1.0 bb= 1.5 K=27.7 n = 0.045

	Louie Rd. (RM 33.92)	DWR (RM 15.5)	Anderson Grade (RM 8.03)	Mouth (USGS gage) (RM 0.62)
Mean Bias	0.09	-0.10	-0.67	-0.95
Mean absolute error (MAE)	0.60	0.77	1.40	1.76
Root mean squared error (RMSE)	0.74	1.00	1.73	2.15
number of hours in sample	168	168	168	168

9.3 Maximum Photosynthetic and Respiration Rate

To assess sensitivity to photosynthetic rates a suite of simulations were completed varying $P_{\max} \pm 0.25$ percent globally (see Figure 13 and Table 13 for baseline values) while holding R constant. Four locations were examined: Louie Road, DWR Weir, Anderson Grade, and the mouth. The impacts on hourly dissolved oxygen for the August 28 through September 4, 2002 period are shown in Figure 43 through Figure 50. When maximum photosynthetic rate is decreased 25 percent (PFAC = 0.75), daily maximum dissolved oxygen values are decreased by approximately 1.0 mg/l at all locations except the mouth, where presumably mechanical reaeration and lower overall standing crop results in a smaller response (well under 0.5 mg/l). Increasing maximum photosynthetic rate by 25 percent (PFAC = 1.25) results in the daily maximum dissolved oxygen values

increasing by approximately 1.0 mg/l at all locations except the mouth, where presumably mechanical reaeration and lower overall standing crop results in a smaller response (approximately 0.5 mg/l). in both cases the Anderson Grade site shows a smaller response than the DWR Weir and Louie Road locations. Overall dissolved oxygen is sensitive when maximum specified photosynthetic rates are increased or decreased 25 percent.

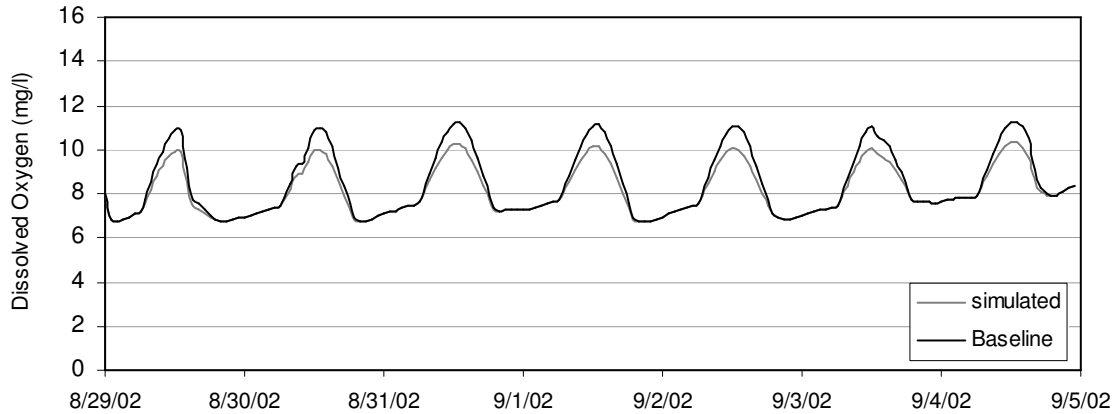


Figure 43. Dissolved oxygen at Louie Rd, PFAC = 0.75: 8/29/02 to 9/5/02

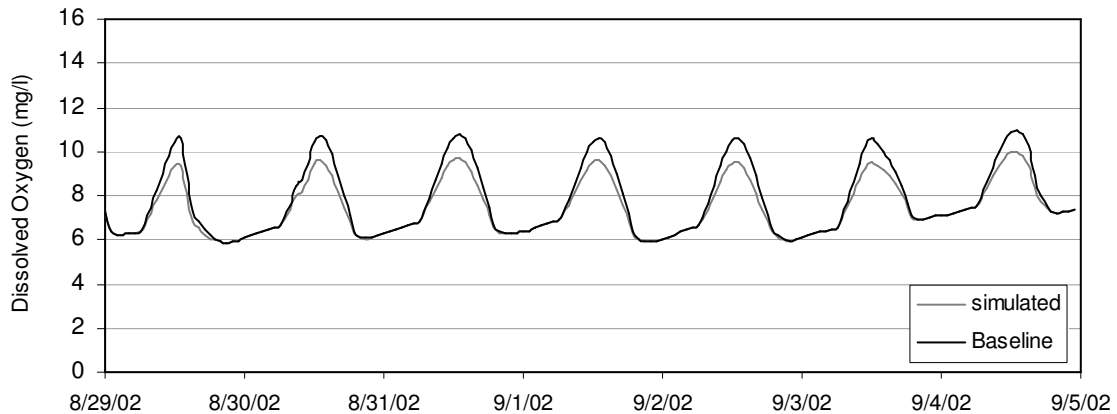


Figure 44. Dissolved oxygen at DWR Weir, PFAC = 0.75: 8/29/02 to 9/5/02

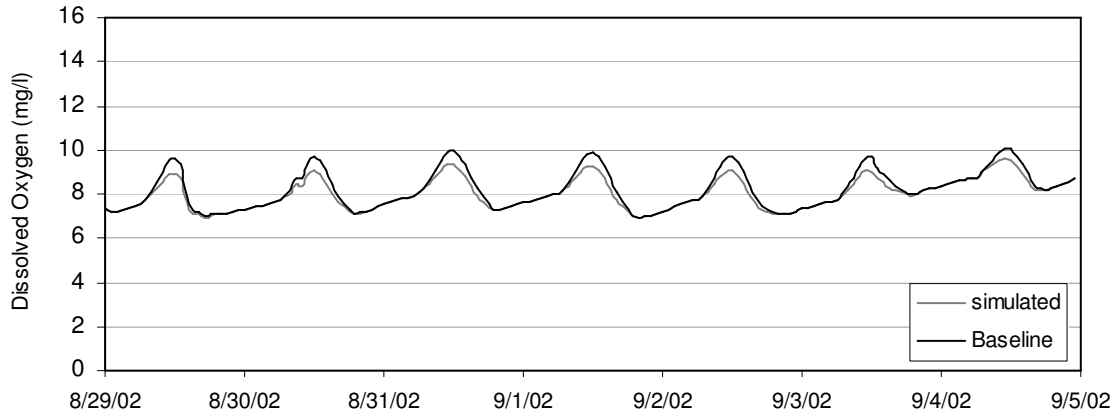


Figure 45. Dissolved oxygen at Anderson Rd, PFAC = 0.75: 8/29/02 to 9/5/02

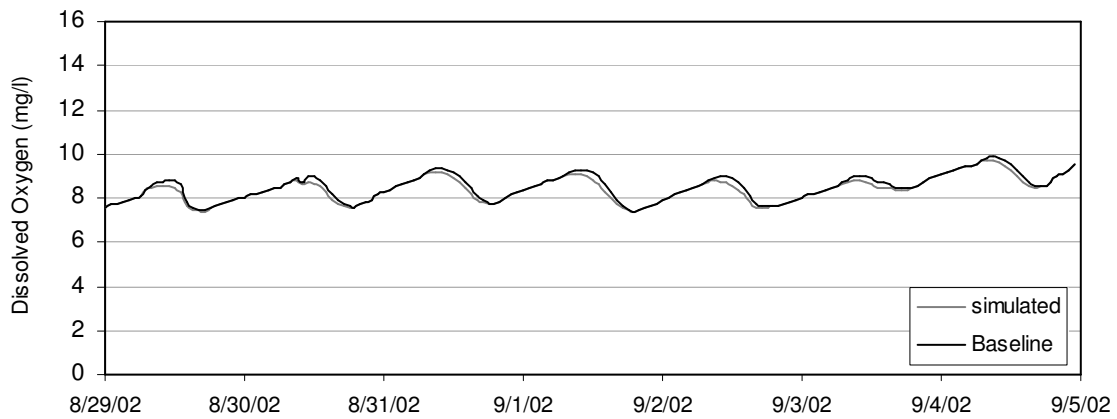


Figure 46. Dissolved oxygen at Mouth, PFAC = 0.75: 8/29/02 to 9/5/02

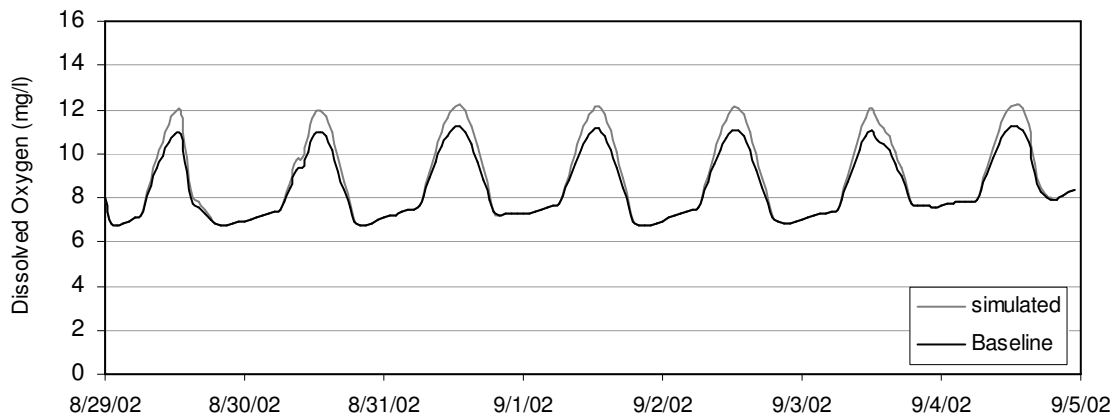


Figure 47. Dissolved oxygen at Louie Rd, PFAC = 1.25: 8/29/02 to 9/5/02

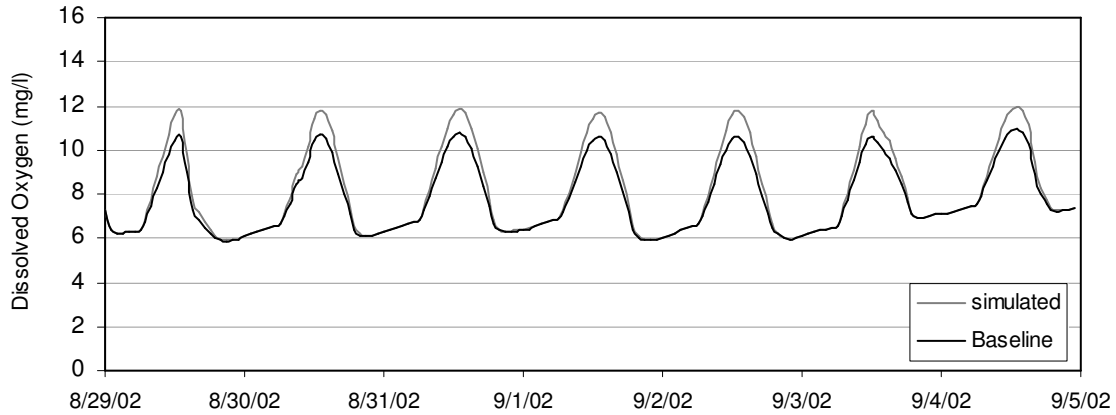


Figure 48. Dissolved oxygen at DWR Weir, PFAC = 1.25: 8/29/02 to 9/5/02

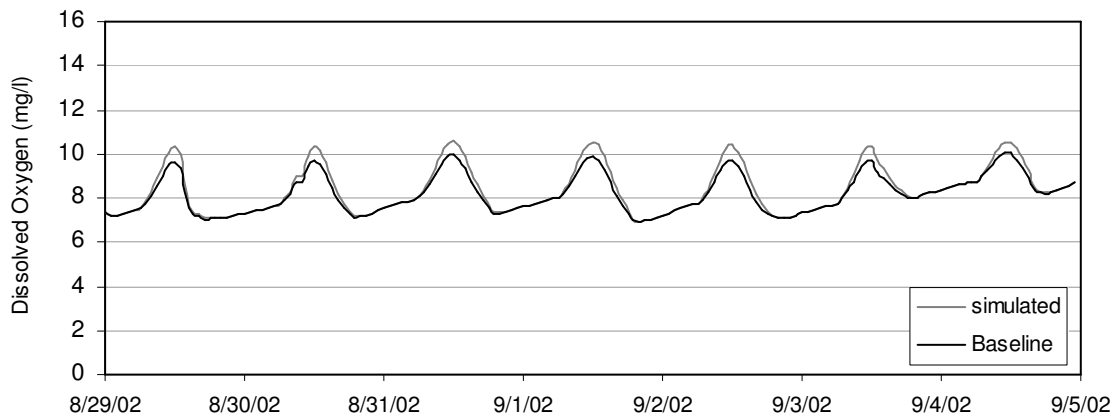


Figure 49. Dissolved oxygen at Anderson Rd, PFAC = 1.25: 8/29/02 to 9/5/02

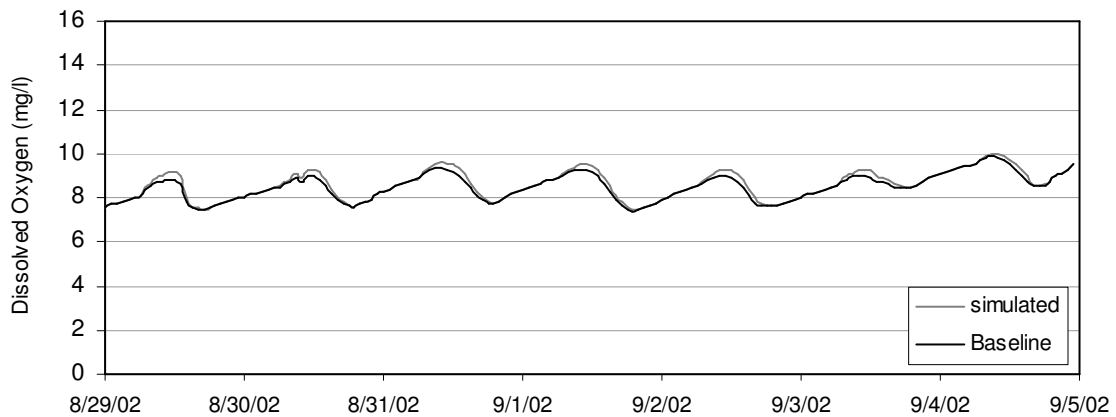


Figure 50. Dissolved oxygen at Mouth, PFAC = 1.25: 8/29/02 to 9/5/02

9.4 CBOD, NBOD, and SOD

The sensitivity of decay coefficients for CBOD and NBOD, as well as SOD rates were assessed using the calibrated model for the period August 29 to September 4. Four locations were examined: Louie Road, DWR Weir, Anderson Grade, and the mouth.

CBOD rates were varied ± 0.1 units from the baseline value of 0.2/d, yielding a range of values from 0.1/d to 0.3/d. Due to low CBOD concentrations in the system, less than 3.5 mg/l on average, the model was insensitive to this range of decay rates with differences of less than 0.1 mg/l at all locations (less than 0.1 mg/l increase with lower decay rates, and less than 0.1 mg/l decrease with higher decay rates).

NBOD rates were increased +0.2 units from a baseline of 0.2 /d. The response was less than a 0.1 mg/l decrease in DO at all locations. As with CBOD, the system has low overall NBOD concentrations, with a system wide average around 2 mg/l. Thus, the impacts of increased decay rates are modest.

SOD was changed to from variable demands ranging from 0.1 g/m² d to 2.0 g/m² d throughout the entire river reach. This had a locally larger effect with DO decreasing by up to approximately 0.2 mg/l at the Anderson Grade location, but overall the impact was modest.

In sum, the impact of sensitivity due to these oxygen demands was small. The low constituent concentrations and overall low SOD values play a role in this insensitivity. However, this does not mean that there are locations where conditions may illustrate a larger impact or that under different hydrologic or loading conditions that the system may show a larger sensitivity.